ESTIMATING HYDRAULIC PROPERTIES OF LANDFILL WASTE USING MULTI STEP DRAINAGE EXPERIMENTS

by

Vincent J. Scicchitano

A thesis submitted to the Faculty of the University of Delaware in partial fulfillment of the requirements for the degree of Master of Civil Engineering

Summer 2010

ESTIMATING HYDRAULIC PROPERTIES OF LANDFILL

WASTE USING MULTI STEP DRAINAGE EXPERIMENTS

by
Vincent J. Scicchitano

Approved: _____
Paul T. Imhoff, Ph.D.
Professor in charge of thesis on behalf of the Advisory Committee

Approved: _____
Harry W. Shenton III, Ph.D.
Chair of the Department of Civil and Environmental Engineering

Approved: _____
Michael J. Chajes, Ph.D.
Dean of the College of Engineering

Approved: _____
Debra Hess Norris, M.S.
Vice Provost for Graduate and Professional Education

ACKNOWLEDGMENTS

I would like to begin by thanking my advisor, Paul Imhoff, and Byunghyun Han, who I like to think of as my second advisor. They have both provided me with much needed direction, and instruction during my time working on this project. I would also like to thank my family and the other students in the lab who provided me with support and help when I needed it. Lastly, I would like to thank the U.S. Department of Energy, who provided funding for this project under Cooperative Agreement DE-FC26-05NT42432 and under Contract No. DE-AC02-05CH11231.

TABLE OF CONTENTS

LIST OF TABLES vi
LIST OF FIGURES viii
ABSTRACT xi

Chapter

1 Introduction 1

2 Column tests on newspaper packings at higher compression 4
2.1 Background 4
2.2 Materials and Methods 5
2.2.1 Column design 5
2.2.2 Column preparation 5
2.2.3 Drainage and multi step outflow tests 6
2.2.4 Saturated hydraulic conductivity test 7
2.2.5 Porosity test 8
2.3 Results 8
2.3.1 Saturated hydraulic conductivity and porosity 8
2.3.2 Drainage and multi step outflow 10
2.3.2.1 Single porosity modeling 11
2.3.2.2 Dual permeability modeling 12
2.3.3 Capillary pressure – volumetric water content – permeability relationship 14
2.4 Summary and Conclusions 15

3 Column tests on real waste samples 29
3.1 Background 29
3.2 Materials and Methods 31
3.2.1 Column design 31
3.2.2 Column preparation 32
3.2.3 Saturated hydraulic conductivity test 35
3.2.4 Drainage tests 35
3.2.5 Porosity test 36
3.3 Results 37
3.3.1 Saturated hydraulic conductivity and porosity 37
3.3.2 Drainage 40

3.3.2.1 Single porosity modeling 41
3.3.2.2 Fracture domain modeling 42
3.3.3 Capillary pressure – volumetric water content – permeability relationship 43
3.4 Validation of porosity testing methods 43
3.5 Summary and Conclusions 44

4 Conclusions 66

Appendix

A Pictures taken while packing the real waste columns 73

LIST OF TABLES

Table 2.1 Packing properties for columns A, B, and C 17

Table 2.2 The water pressure heads and capillary pressure heads for pressure steps at the bottom boundary for column C. "G" indicates gravity drainage, while "M" indicates multi step outflow. 17

Table 2.3 Hydraulic conductivity results from the idealized waste and literature values for other waste samples 18

Table 2.4 Weights associated with each data point used in the HYDRUS-1D modeling for column C 18

Table 2.5 Hydraulic parameters optimized with the HYDRUS-1D single porosity model for columns A, B, and C (± values show the 95% confidence interval)..... 19

Table 2.6 Hydraulic parameters optimized with the HYDRUS-1D dual permeability model for columns A, B and C (± values show the 95% confidence interval)..... 20

Table 3.1 Waste generation, recovery and disposal based on the USEPA (2009) study in millions of tons (assumed to be air dried)..... 46

Table 3.2 Waste composition for RWA, RWB, RWC and RWD (weights are air dried) 46

Table 3.3 Packing properties for the four samples that were tested..... 47

Table 3.4 The water pressure heads for pressure steps at the bottom boundary for RWA, RWB, RWC, and RWD. "G" indicates gravity drainage. 47

Table 3.5 Hydraulic conductivity and effective porosity results from this study on real waste and literature values for other waste samples 48

Table 3.6 Hydraulic parameters optimized with the HYDRUS-1D single porosity model for the real waste samples (± values show the 95% confidence interval)..... 49

Table 3.7 Comparison of hydraulic parameters from the literature with those found in this study..... 49

Table 3.8 Hydraulic parameters of the fracture domain optimized with the HYDRUS-1D single porosity model for the real waste samples (± values show the 95% confidence interval) 50

LIST OF FIGURES

Figure 2.1 Diagram of the experimental column used in the newspaper tests (Han, 2009) 21

Figure 2.2 Detailed design of the bottom plate used in the newspaper tests (Han, 2009) 22

Figure 2.3 The change in saturated hydraulic conductivity with flow rate for column C. 23

Figure 2.4 Outflow flux data for column C with inverse modeling fits using the best fit parameters from Tables 2.5 and 2.6. 24

Figure 2.5 Water pressure data for column C with inverse modeling fits using the best fit parameters from Tables 2.5 and 2.6. 24

Figure 2.6 Comparison of the fitted residual water content of the matrix domain for columns A, B and C. 25

Figure 2.7 Comparison of the fitted alpha value of the matrix domain for columns A, B and C. 25

Figure 2.8 Comparison of the fitted n value of the matrix domain for columns A, B and C. 26

Figure 2.9 Comparison of the fitted saturated hydraulic conductivity value of the matrix domain for columns A, B and C. 26

Figure 2.10 The capillary pressure-volumetric water content relationships for columns A, B, and C. The lines show the best fit model predictions for the single porosity (upper plot) and dual permeability (lower plot) models. 27

Figure 2.11 Permeability-volumetric water content relationship for Column C. 28

Figure 3.1 Diagram of the experimental columns used in the real waste tests 51

Figure 3.2 Diagram of the manifold used to convey outflow in the real waste tests. 52

Figure 3.3 The change in saturated hydraulic conductivity with flow rate for the real waste columns 53

Figure 3.4 Outflow flux data for RWA (upper plot) and RWB (lower plot) with inverse modeling fits using the best fit parameters from Table 3.6. (Figure 3.3 continued on the following page)..... 54

Figure 3.4 Outflow flux data for RWC (upper plot) and RWD (lower plot) with inverse modeling fits using the best fit parameters from Table 3.6..... 55

Figure 3.5 Water pressure data for RWA (upper plot) and RWB (lower plot) with inverse modeling fits using the best fit parameters from Table 3.6 (Figure 3.4 continued on the following page)..... 56

Figure 3.5 Water pressure data for RWC (upper plot) and RWD (lower plot) with inverse modeling fits using the best fit parameters from Table 3.6..... 57

Figure 3.6 Outflow flux data for RWA (upper plot) and RWB (lower plot) with inverse modeling fits using the best fit fracture parameters from Table 3.8. (Figure 3.5 continued on the following page) 58

Figure 3.6 Outflow flux data for RWC (upper plot) and RWD (lower plot) with inverse modeling fits using the best fit fracture parameters from Table 3.8. 59

Figure 3.7 Water pressure data for RWA (upper plot) and RWB (lower plot) with inverse modeling fits using the best fit fracture parameters from Table 3.8 (Figure 3.6 continued on the following page) 60

Figure 3.7 Water pressure data for RWC (upper plot) and RWD (lower plot) with inverse modeling fits using the best fit fracture parameters from Table 3.8 61

Figure 3.8 The capillary pressure-volumetric water content relationships for RWA (upper plot) and RWB (lower plot). The lines show the best fit model predictions for the single porosity models (Figure 3.7 is continued on the next page) 62

Figure 3.8 The capillary pressure-volumetric water content relationships for RWC (upper plot) and RWD (lower plot). The lines show the best fit model predictions for the single porosity models 63

Figure 3.9 Comparison of the capillary pressure-volumetric water content curves developed in this study with curves found in the literature (The red dotted line is an approximation of the highest capillary pressure measured by Kazimoglu, 2006.) 64

Figure 3.10 Permeability-volumetric water content relationship for the real waste column tests 65

Figure A.1 Mixed waste prior to packing 73

Figure A.2 Mixed waste in the column prior to compression 74

Figure A.3 Compressing the column 75

Figure A.4 Waste after compression 76

Figure A.5 Completely compressed waste column with top plate and support rods 77

ABSTRACT

Laboratory tests were conducted on two types of waste samples in order to explore how the hydraulic properties and constitutive relationships of waste samples can vary. The first waste sample was idealized and composed entirely of newspaper. The second set of samples was made up of components typically found in municipal solid waste landfills. The tests used were developed by Han (2009) and performed as a continuation of his research. Saturated hydraulic conductivity, drainage, multi step outflow, and porosity tests were performed on a newspaper sample similar to those used by Han (2009), but packed to a higher compaction density. The results of those tests supported conclusions drawn by Han (2009). First, a dual permeability model is needed to accurately describe the hydraulic behavior of an idealized waste sample and it is likely that such a model would be necessary to describe real waste. Second, although physical manipulations of the waste (i.e. changing the compaction density) can alter the fracture properties of the waste significantly, there is very little variation in the matrix properties of the waste. This suggests that the matrix domain of landfilled waste should be similar if the compositions of porous materials in the landfills are similar.

Four real waste samples with very similar compositions were studied using modified versions of the saturated hydraulic conductivity, drainage, and porosity tests developed for the newspaper samples. The data collected from the tests was inversely modeled using HYDRUS-1D and one of two assumptions. First, it could be

assumed that the pore structure of the waste could be described by a single pore domain model. The second assumption was that the waste was better described as a dual domain system and the behavior observed in the drainage tests could be used to describe only the fracture domain. There was some variability observed among the hydraulic parameters and constitutive relationships of the four tests in this study, and a great deal more variability when the results were compared with similar studies in the literature.

Chapter 1

INTRODUCTION

Bioreactor landfills are designed to allow for optimal moisture content for biological growth. The most common process used to achieve optimal moisture is leachate recirculation. Leachate produced in the landfill is recycled as needed to provide suitable conditions which allow for a more rapid and complete waste degradation when compared to the traditional dry tomb landfilling approach (Reinhart and Townsend, 1998). A brochure distributed by Waste Management has suggested that as much as 15 – 35% of the space in a typical landfill can be recovered as the waste decomposes into gases. This extra space can be reused, thus limiting the need to build new landfill facilities. In addition to faster stabilization and decomposition rates, the reuse of leachate helps to minimize leachate disposal and management costs.

In order to properly design a bioreactor landfill, it is first necessary to know what the optimal moisture conditions are for biological growth and how to reach those optimal conditions. An accurate understanding of how fluids (both gases and liquids) flow through the solid waste in a landfill is required if optimal moisture conditions are to be reached. This understanding can come from applying multiphase modeling techniques used for soil systems to solid waste (Han, 2009).

In order to solve the multiphase equations, constitutive relationships must be developed that can describe the flow properties of the waste. The hydraulic conductivity of solid waste has been studied in depth and many measurements of this property are available in the literature (Powrie and Beaven, 1999; Chen and

Chynoweth, 1995; Durmusoglu et al., 2006). However, other properties such as the porosity (Korfiatis et al., 1984; Bleiker et al., 1993) or the pressure saturation relationship (Kazimoglu et al., 2006) of solid waste are less prevalent.

Modeling of these constitutive relationships can be done in two different ways. One option is to use a single porosity model which assumes a single homogeneous pore structure throughout. The other, which more accurately represents the pore structure of a landfill, is the dual permeability model. This model assumes a dual domain pore structure that is made up of a fracture domain (macropores) between solid waste particles and a matrix domain (micropores) within the materials of the solid waste. Studies such as Johnson et al. (2001) have shown that this dual domain assumption is necessary to accurately portray the preferential water flow that has been observed in laboratory and field studies of landfills (Johnson et al., 1998; Rosqvist et al., 2005).

Even though it has been shown that a dual domain pore structure is more useful in describing preferential fluid flow through a landfill, difficulties in obtaining the necessary parameters for a dual domain description have limited modeling efforts to single domain descriptions. Han (2009) developed a number of tests (saturated hydraulic conductivity, drainage, multi step outflow, porosity and gas permeability) using a homogeneous “waste” sample composed of newspaper to develop constitutive relationships which could assume either a single domain or a dual domain description.

The tests by Han (2009) investigated the effect of the size of waste particles in homogeneous samples on different model flow parameters. That work is continued and expanded in this study to explore the effects that were not previously tested. The same experimental procedure was used in this study to determine what the

effects would be when a higher compression was used on the homogeneous newspaper waste sample. The same experimental procedure was then modified to test how model parameters varied when a heterogeneous sample of real solid waste was used instead of an idealized homogeneous waste.

Chapter 2

COLUMN TESTS ON NEWSPAPER PACKINGS AT HIGHER COMPRESSION

2.1 Background

In order to develop constitutive relationships for the idealized newspaper waste sample, transient water flow data are required. The drainage and multi step outflow (MSO) tests can provided these transient data. These data were collected in earlier work for newspaper samples with different particle sizes (Han, 2009). Once the time variable data were obtained, they were fit with two different HYDRUS-1D (Šimůnek et al., 2008) inverse models – single porosity and dual permeability. The single porosity model assumes one homogeneous pore system, while a dual permeability model allows for the flow and transfer of water through and between a large fracture domain (macropores) and a matrix domain (micropores). The inverse models provided important parameters necessary for describing the flow of water through these newspaper packings. More importantly, this modeling exercise provides insight into the effect of refuse particle size on fluid flow in landfills and the necessity of dual domain descriptions of fluid flow.

The use of a higher compression density of a newspaper packing in this study was used to see how the flow properties of a landfill might change with increasing depth. As depth increases in a landfill, the self weight of the waste placed above causes higher compression rates (Bleiker et al., 1993). It is important not only to understand what happens at the surface of a landfill, but also at higher depths.

Due to the fact that this test is a continuation of previous work completed by Han (2009) and most materials and methods are the same, only cursory details are presented with particular emphasis on any procedures that differed from that earlier work. For further details on any of these procedures, the reader should refer to the work by Han (2009).

2.2 Materials and Methods

2.2.1 Column design

An experimental column designed and built by Han (2009) was used to conduct the experiment. The column was based on a similar design by Hopmans et al. (1998), and altered to allow for larger volumes of refuse, different compaction densities and for saturated hydraulic conductivity, drainage, multi step outflow, and porosity tests on the same sample without any disturbance.

The schedule-80 PVC column is 70 cm long with an internal diameter of 29 cm. The column has three sections, each separated by a 1.3 cm aluminum plate with openings to allow for water or gas flow. The top and bottom sections allow for water and gas injection into the column and the middle section contains the compacted sample and testing ports. A detailed schematic of the column and bottom plate is shown in Figures 2.1 and 2.2.

2.2.2 Column preparation

The preparation of the higher compaction newspaper column (hereafter known as column C) followed the procedure laid out by Han (2009) with some minor differences. Once again, newspaper from the University of Delaware student paper "The Review" was used as the sample. As in the case of column A (Han, 2009), each

sheet of newspaper was cut into eighths (17.9 cm W × 14.5 cm L) and then crumpled by hand and air dried. In the previous test, the newspaper was distributed evenly into four bags with approximately 225 g in each bag. For column C, six bags of newspaper (again weighing approximately 225 g each) were used. During the compaction process, each bag was poured into the column and compressed at 45 kPa instead of 30 kPa, thereby compacting column C to approximately one and a half times the density of columns A and B (Han, 2009). Table 2.1 shows the packing properties of column C as well as the properties of columns A and B from the previous work by Han (2009).

After packing the columns, ceramic cup tensiometers were inserted into the sample through ports in the wall of the column and the samples were flushed with DI water until the water exiting the column was clear. The sample was then saturated by injecting CO_2 gas at the bottom of the sample at a flow rate of 5 LPM for one hour, then applying a 0.7 atm vacuum to the top of the column, and injecting degassed water into the bottom of the column at 0.22 L/min for one hour and fifteen minutes and then increasing the flow to 0.44 L/min for another 30 minutes.

2.2.3 Drainage and multi step outflow tests

The drainage and multi step outflow experiments recorded four measurements continuously for the duration of the tests. These measurements were: gas pressure, measured with a pressure sensor connected to the upper chamber of the column with empty tubing; capillary pressures at two points in the sample, measured with pressure sensors connected to ceramic cups drilled into the sample by water filled tubing; and the volume of water flowing out of the column, measured by a reservoir on a balance.

A system of valves on the outflow lines allowed the water coming out of the column at the bottom to flow either through the nylon membrane or through holes in the bolts securing the membrane. The drainage test was gravity driven with no applied gas pressure, and the water allowed to flow through the holes in the bolts. The boundary conditions for the different steps in the drainage test were controlled by changing the height of the outflow tube.

Immediately following the drainage test, a multi step outflow test was performed. For this test the water was allowed to drain through the nylon membrane instead of through the bolt holes. The boundary conditions for this test were controlled by setting the height of the outflow tubing to the bottom of the sample and increasing the gas pressure for each new step by injecting nitrogen gas into the top chamber of the column. The boundary conditions for each step are shown in Table 2.2.

2.2.4 Saturated hydraulic conductivity test

The saturated hydraulic conductivity test was performed after the MSO test. The column was re-saturated using the same procedure used to saturate the sample before the drainage test, but allowing excess water above the top of the sample. The water was then recirculated from the bottom chamber to the top chamber using a peristaltic pump. The flow rate was monitored and changed incrementally using two flow meters ranging from 60 mL/min to 3000 mL/min. At each flow increment, the flow was allowed to stabilize. At this point, the pressure gradient between tubing inserted at one of the monitoring ports in the waste sample and tubing inserted into the upper chamber of the column was recorded. Darcy's law was then

used along with the recorded flow rates and pressure gradients to calculate the saturated hydraulic conductivity.

2.2.5 Porosity test

After performing the saturated hydraulic conductivity test, the sample was again re-saturated. The drainage test was rerun, this time including only the first multi step outflow step (M0). The cumulative outflow was monitored and represents the water released from the largest pores in the waste sample. Following the drainage test, the wet sample was removed from the column, weighed, and allowed to dry in an oven at 95 °C until the rest of the water had evaporated out of the sample. To ensure that all water was evaporated, the sample was weighed before it was put into the oven and after it was taken out each day. When the weight of the sample after drying was the same for two days in a row, it was assumed that all water was removed. The total volume of water in the sample was determined by summing the water drained from the column and the water evaporated in the oven. The total porosity of the sample was then calculated as the total volume of water in the sample divided by the total volume of the column.

2.3 Results

2.3.1 Saturated hydraulic conductivity and porosity

To determine the hydraulic conductivity, it is first necessary to ensure that Darcy's law is valid. As seen in Figure 2.3, and consistent with the results from Han (2009), there is a decrease in hydraulic conductivity as the flow rate increases. This implies friction losses that do not occur if the flow is laminar, which it must be for Darcy's law to apply.

In order to verify that Darcy's law was valid, the waste sample was considered a bed packed with spherical media. Seguin et al. (1998) suggested that beds packed with spherical media have a laminar flow region ending at a pore Reynolds number of approximately 180. Using the following equation as suggested by Seguin et al. (1998) and used by Han (2009), the pore Reynolds number could be computed.

$$Re_{pore} = \frac{q_w \cdot d}{(1-w_f) \cdot v} \tag{2.1}$$

where Re_{pore} is the pore Reynolds number for a bed packed with spherical media [-], d is the mean particle diameter [L], w_f is the volumetric fraction of fracture [-], and v is the kinematic viscosity of water [L^2T^{-1}]. For column C, the particle diameter was estimated to be 5 cm. By assuming that the water draining from steps G1 to M1 came primarily from the fractures or large pores between the pieces of newspaper and that the water draining from steps M2 to M5 was drained from the matrix, the fraction of pore space which is made up of fractures, w_f, can be calculated as the volume of water that came out at the end of step M1 divided by the total volume of the sample. This value was 0.4256 for column C.

Using the equation above, Darcy's law seems to be valid for all of the points in Figure 2.3 which have pore Reynolds numbers ranging from 1.5 to 76.0. Due to the difficulty in accurately recording pressure gradients at Darcy fluxes less than 0.017 cm/sec, and the apparent viscous losses at higher flow rates, the hydraulic conductivity of 1.16 cm/min, or 1.94 x 10^{-4} m/s was determined using a Darcy flux of 0.017 cm/sec (Re_{pore} = 15.2).

It is interesting to note that an increase in the density by a factor of 1.5 results in a hydraulic conductivity almost 20 to 100 times smaller, depending on the

particle size, than the original samples tested by Han (2009). A similar test performed by Chen and Chynoweth (1995), which tested the hydraulic conductivity of a paper and plastic refuse-derived fuel packed to densities of 160, 320, and 480 kg/m^3 resulted in hydraulic conductivities ranging from 0.8 – 7.0 cm/min. The value of 1.16 cm/min obtained in this study (from a sample packed to a density of 210 kg/m^3) agrees well with the findings of Chen and Chynoweth (1995). Table 2.3 shows how the saturated hydraulic conductivity of column C compares with various other studies on solid waste.

The total porosity of the sample in column C was $\varepsilon = 0.887$. This value is lower than columns A and B from Han (2009), which were $\varepsilon = 0.934$ and $\varepsilon = 0.936$, respectively. This is expected due to the higher compaction density of column C. It also shows that much of the porosity of a newspaper sample is due to the matrix, or the pores of the newspaper itself since the higher compaction resulted in a relatively small decrease in porosity.

2.3.2 Drainage and multi step outflow

After the data for outflow, water pressure and gas pressure were recorded: 21 evenly spaced data points were chosen for each pressure step based on the total outflow for each step. The water pressures were converted to capillary pressures by subtracting the measured water pressure from the applied gas pressure and the cumulative outflow data was divided by the area of the column to get cumulative outflow flux data. This data was then inversely modeled using the HYDRUS-1D program. For steps G1 to M0, however, only the final data point was used. The transient data was not used because it was unclear whether or not the tubing and connections on the outflow line were controlling the rate at which the water drained.

The final data point that was used represents the condition at which all of the water had been drained for each step.

2.3.2.1 Single porosity modeling

In order to achieve the best overall fit to all of the pressure steps, the data from each step were weighted the same. Since there was only one data set for outflow, but two data sets for pressure (one from each tensiometer), the data for the pressure readings were weighted half as heavily as the outflow data. For the last step, which had only 13 data points, the weighting for each data point was increased to give the same overall weight as the other steps. Table 2.4 shows how each step was weighted for the pressure and outflow data.

Using the single porosity model in HYDRUS-1D, there are six parameters that the user needs to fit: θ_{wr}, the residual water content; θ_{ws}, the saturated water content; α and n, the van Genuchten parameters; K_s, the saturated hydraulic conductivity; and l, the tortuosity. The more parameters the user fixes, the better HYDRUS-1D is able to converge on a unique solution. In order to reduce the number of fitted parameters, the saturated water content was set equal to the total porosity of the waste sample, the saturated hydraulic conductivity was set equal to the independently measured value found above, and the tortuosity parameter was assumed to be 0.5. This assumption is commonly made by soil scientists (Kodešová et al., 2008; Köhne et al., 2005). The rest of the parameters (θ_{wr}, α and n) were fitted by HYDRUS-1D.

The fitted parameters for this study and the previous work by Han (2009) can be seen in Table 2.5 along with their 95% confidence intervals. The single porosity model fits to the outflow and water pressure data can be seen in Figures 2.4

and 2.5, respectively. As with the previous work by Han (2009), the model fit to the outflow data is relatively good for the single porosity model. However, the model does not fit the water pressure data well.

2.3.2.2 Dual permeability modeling

In an attempt to improve the fit of the single porosity, a dual permeability model was employed. Using the model suggested by Gerke and van Genuchten (1993) in HYDRUS-1D, there are 17 parameters needed as opposed to the six needed for the single porosity model. To reduce the number of unknown parameters, the following assumptions used by Han (2009) were used.

The first assumption relates to fraction of pore space which is made up of fractures and was presented in Section 2.3.1. Again, the variable w_f was 0.4256 for column C. Using this assumption, the saturated water content of the matrix domain, θ_{wsm}, can be estimated as

$$\theta_{wsm} = \frac{\varepsilon - w_f \cdot \theta_{wsf}}{1 - w_f} \tag{2.2}$$

The saturated water content of the matrix domain for column C was calculated to be $\theta_{wsm} = 0.8036$.

Since the fractures are large and there are no smaller particles in the waste sample, it can be assumed that the saturated water content of the fractures, θ_{wsf}, is equal to one. Similarly, because of the large size of the fractures, it can be assumed that the water is drained from them at relatively low capillary pressures and the residual water content of the fracture domain, θ_{wrf}, can be set to zero. Since most of the water flows though the fracture domain when the sample is saturated, the saturated hydraulic conductivity of the fracture domain, K_{sf}, can be calculated by dividing the

bulk saturated hydraulic conductivity that was measured independently, K_s, by the volume fraction of fractures, w_f.

The tortuosity parameters for the fracture and matrix domains, l_f and l_m, were both set to 0.5. A shape factor dependent on the geometry, β, was set to 8, the midpoint between the values for a rectangular slab and a sphere. An empirical scaling factor, γ, was set at 0.4. The distance from the center of a matrix block to the fracture, was measured as 2.5 cm and K_a, the effective hydraulic conductivity of the fracture-matrix interface was set to 10^{-4} cm/hr. All of these values were either measured or set as they are to be consistent with the previous modeling performed by Han (2009).

The van Genuchten parameters for the fracture domain, α_f and n_f, were obtained by using an inverse single porosity model on steps G1 to M0. It is assumed that the fracture domain dominates during these first steps and by modeling them as a single domain, the van Genuchten parameters that are fitted would be for the fracture domain only. The four parameters left are the residual water content of the matrix domain, θ_{wrm}, the van Genuchten parameters for the matrix domain, α_m and n_m, and the saturated hydraulic conductivity of the matrix domain, K_{sm}. These four parameters were all fitted using inverse modeling and the outflow and pressure data collected from the drainage and MSO tests.

The parameters resulting from the dual permeability modeling can be seen along with those observed by Han (2009) in Table 2.6 and the model fits to the outflow and water pressure data can be seen in Figures 2.4 and 2.5.The R^2 value for the dual permeability model (R^2 = 0.9981) shows a slight improvement over the single porosity model (R^2 = 0.992). Visually, however, the fits to the outflow and water pressure data are very good. The dual permeability model used to fit the outflow data

shows a small improvement over the single porosity model, and a significant improvement over the single porosity model for the water pressure data.

Han (2009) showed that by changing the size of the newspaper balls, there were large differences in the saturated hydraulic conductivity and the fracture parameters fitted by HYDRUS-1D. However, the size difference did not affect the matrix parameters. Comparing the fitted parameters from column C to columns A and B from Han (2009), this point is reinforced. Despite a higher compaction density and a much smaller saturated hydraulic conductivity, it can be seen clearly from Figures 2.6, 2.7, 2.8 and 2.9 that the matrix parameters from this study still fall within the 95% confidence intervals of the previous study by Han (2009). These findings support the argument that the matrix domain does not change when a waste sample (at least an idealized one) is subjected to different physical conditions. These different physical conditions can, however, play a large role in changing the properties of the fracture domain.

2.3.3 Capillary pressure – volumetric water content – permeability relationship

The capillary pressure – volumetric water content data and fitted curves for the single porosity and dual permeability models can be seen in Figure 2.10 along with the data from Han (2009) for comparison. The data points for this curve were taken from the endpoints of each step of the drainage and multi step outflow tests. As can be seen in Figure 2.10, the dual permeability model again shows a better fit than the single porosity model, especially in the range $0.2 \leq \theta_w \leq 0.4$.

Despite the similarities among the matrix parameters for all three columns, column C shows a different capillary pressure-volumetric water content relationship. Columns A and B, though packed with different size waste particles,

showed very similar capillary pressure-volumetric water content relationships. However, when a sample is compressed to a higher density, as in the case for column C, it has a lower water content at saturation and a higher water content everywhere else. This would seem to be a reasonable result since a higher density sample would contain a higher fraction of water in the matrix domain. This water is not as easily drained as the fractures, and would be retained for a higher water content throughout the test.

The permeability-volumetric water content curves for columns A, B and C can be seen in Figure 2.11. The curves for column C show a large difference between the two model fits. This is similar to what Han (2009) observed in columns A and B. However, where Han observed an almost identical behavior for columns A and B when $\theta_w \leq 0.4$ using the dual permeability model, column C does not fall on the same line. This shows that changing the compaction of the waste sample can have a large effect on the permeability-volumetric water content relationship.

2.4 Summary and Conclusions

Four tests were carried out on an idealized waste sample similar to those that had been tested before by Han (2009). The object of this research was to test how altering the compression density can affect the flow parameters and behaviors of a solid waste sample. After the drainage, multi step outflow, saturated hydraulic conductivity and porosity experiments were carried out, the data were inversely modeled using both a single porosity and a dual permeability model and used to develop constitutive relationships for the newspaper waste samples.

The results of the newspaper tests show that while fracture domains can vary greatly, the matrix domain remains relatively unchanged when the physical

properties of the waste are changed. This suggests that matrix domains for landfilled wastes should be similar as long as the compositions of the porous materials in the landfills are similar. It is also important to note that despite the similarities in the matrix domain, the capillary pressure-volumetric water content relationship can be different. This relationship relies heavily on the density of the waste and shows a higher water content with increasing waste density.

Using an idealized waste sample made up solely of crumpled up newspaper balls makes it easier to see how changes such as waste particle size or compression density affect the flow properties of the waste. The use of newspaper as the ideal waste is justified in that paper products are the most common constituent of landfill waste. This suggests that although the tests performed by Han (2009) and the test in this study are idealized, it is likely that the dual permeability description could be applied to real solid waste as long as a large portion of the waste is made up of porous materials (i.e. paper, textiles, or food and yard wastes). The next chapter of this thesis will discuss experiments run on real waste samples as opposed to idealized newspaper samples.

Table 2.1 Packing properties for columns A, B, and C

	Column A (Han, 2009)	Column B (Han, 2009)	Column C
Diameter of column (cm)	28.4	28.3	28.3
Height of sample (cm)	11	11.6	11.1
Tensiometer installation	2 measurements (2.5 cm and 7.8 cm from sample bottom)	2 measurements (2.6 cm and 8.3 cm from sample bottom)	2 measurements (2.6 cm and 8.3 cm from sample bottom)
Weight of newspaper (g)	901.7	910.3	1469.6
Packing density (kg/m^3)	129	125	210
Compaction Pressure (kPa)	30	30	45
Size of Newspaper	Newspaper sheet cut to 1/8 of original size	Original sheet size (no cutting)	Newspaper sheet cut to 1/8 of original size

Table 2.2 The water pressure heads and capillary pressure heads for pressure steps at the bottom boundary for column C. "G" indicates gravity drainage, while "M" indicates multi step outflow.

Steps	G1[1]	G2[1]	G3[1]	G4[1]	M0[2]	M1[2]	M2[2]	M3[2]	M4[2]	M5[2]
C (cm H_2O)	8.3	5.6	2.8	0	5	45	100	200	400	700

[1] Water pressure head
[2] Capillary pressure head

Table 2.3 Hydraulic conductivity results from the idealized waste and literature values for other waste samples

Author	Hydraulic conductivity (m/s)	Dry Density (kg/m^3)
Scicchitano (2010)	1.93×10^{-4}	210
Han (2009)	3.81×10^{-3} to 1.89×10^{-2}	125 to 129
Chen and Chynoweth (1995)	4.7×10^{-7} to 9.6×10^{-4}	160 to 480
Fungaroli and Steiner (1979)	1×10^{-6} to 1×10^{-4}	100 to 350
Oweis et al. (1990)	1×10^{-5} to 1.5×10^{-6}	-
Burrows et al. (1997)	3.9×10^{-7} to 6.7×10^{-5}	-
Korfiatis et al. (1984)	8×10^{-5} to 1.3×10^{-4}	616
Bleiker et al. (1993)	5×10^{-9} to 1×10^{-6}	500 to 1200

Table 2.4 Weights associated with each data point used in the HYDRUS-1D modeling for column C

Steps	G1	G2	G3	G4	M0	M1	M2	M3	M4	M5
No. of Data Points	1	1	1	1	1	21	21	21	21	13
Weight for outflow	21	21	21	21	21	1	1	1	1	1.62
Weight for pressure	10.5	10.5	10.5	10.5	10.5	0.5	0.5	0.5	0.5	0.81

Table 2.5 Hydraulic parameters optimized with the HYDRUS-1D single porosity model for columns A, B, and C (± values show the 95% confidence interval)

	θ_{wr} [-]	θ_{ws} [-]	α [cm^{-1}]	n [-]	K_s [cm/hr]	l [-]	R^2
A[1]	0.0724 ± 0.0056	0.934	0.482 ± 0.023	1.536 ± 0.023	1373	0.5	0.9685
B[1]	0.005 ± 0.017	0.936	1.026 ± 0.067	1.312 ± 0.022	6797	0.5	0.9931
C	0.0319 ± 0.019	0.8872	0.170 ± 0.0059	1.330 ± 0.029	69.75	0.5	0.992

[1] Tests performed by Han (2009)

Table 2.6 Hydraulic parameters optimized with the HYDRUS-1D dual permeability model for columns A, B and C (± values show the 95% confidence interval)

Matrix							
	θ_{wrm} [-]	θ_{wsm} [-]	α_m [cm^{-1}]	n_m [-]	K_{sm} [cm/hr]	l_m [-]	R^2
A[1]	0.220 ± 0.042[2]	0.808	0.0081 ± 0.0010[2]	1.990 ± 0.023[2]	0.188 ± 0.060[2]	0.5	0.9969[2]
B[1]	0.185 ± 0.071[2]	0.826	0.0085 ± 0.0015[2]	2.12 ± 0.035[2]	0.20 ± 0.11[2]	0.5	0.9956[2]
C	0.2681 ± 0.028[2]	0.8036	0.0080 ± 0.0011[2]	1.975 ± 0.204[2]	0.203 ± 0.044[2]	0.5	0.9981[2]

Fracture							
	θ_{wrf} [-]	θ_{wsf} [-]	α_f [cm^{-1}]	n_f [-]	K_{sf} [cm/hr]	l_f [-]	R^2
A[1]	0	1	0.457 ± 0.013[3]	1.99 ± 0.014[3]	2089	0.5	0.9998[3]
B[1]	0	1	0.722 ± 0.222[3]	1.75 ± 0.23[3]	10713	0.5	0.9992[3]
C	0	1	0.162 ± 0.013[3]	2.04 ± 0.26[3]	387.52	0.5	0.9978[3]

Exchange Terms					
	w [-]	B [-]	γ [-]	a [cm]	K_a [cm/hr]
A[1]	0.657	8	0.4	2.5	0.0001
B[1]	0.634	8	0.4	5	0.0001
C	0.4256	8	0.4	2.5	0.0001

[1] Tests performed by Han (2009)

[2] Estimated from inverse modeling with dual permeability model with fixed a_f and n_f and outflow and water pressure data from G1 to M5 steps.

[3] Estimated from inverse modeling with single porosity model in order to determine a_f and n_f using outflow and water pressure data from G1 to M0 steps.

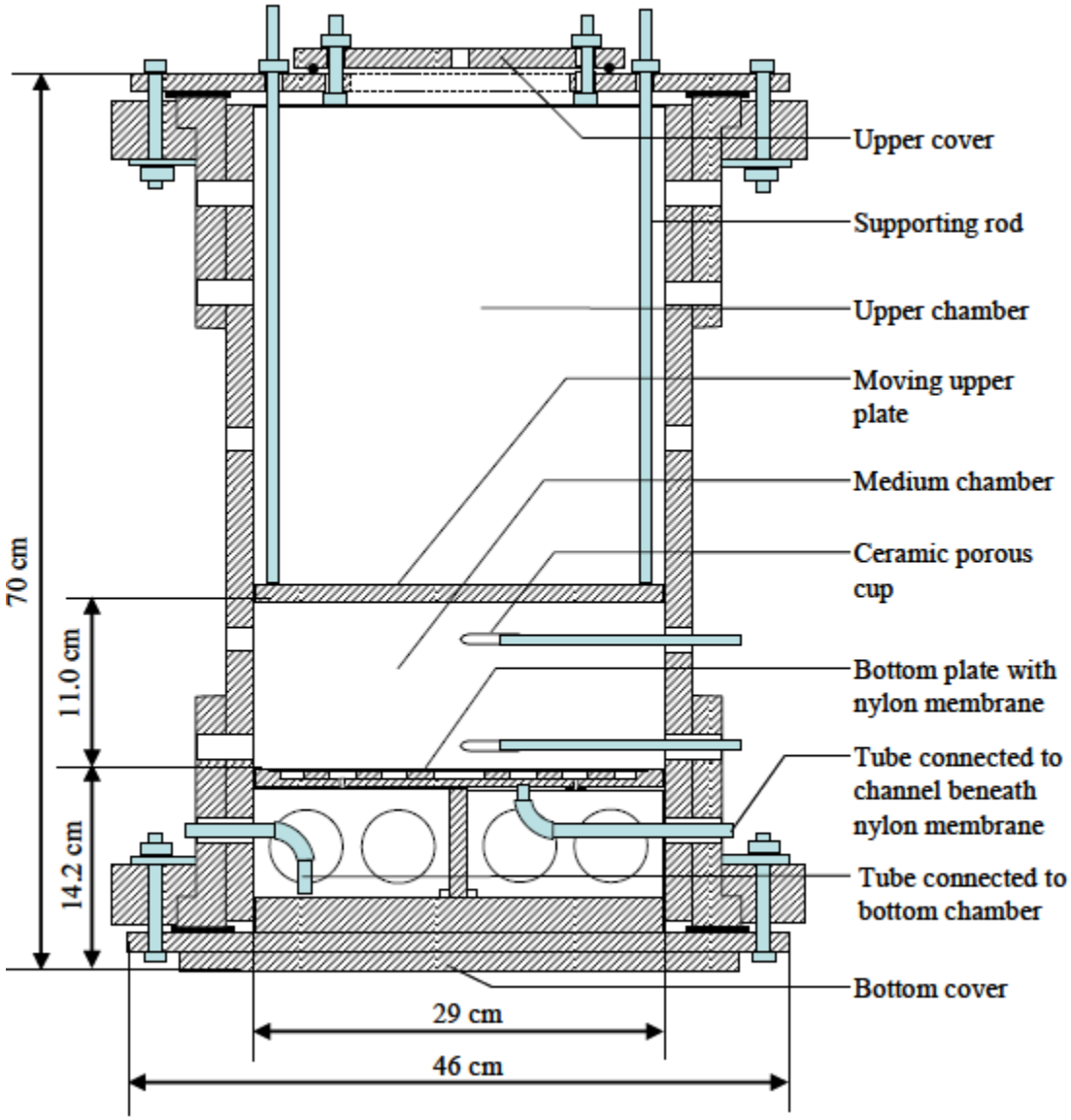

Figure 2.1 Diagram of the experimental column used in the newspaper tests (Han, 2009)

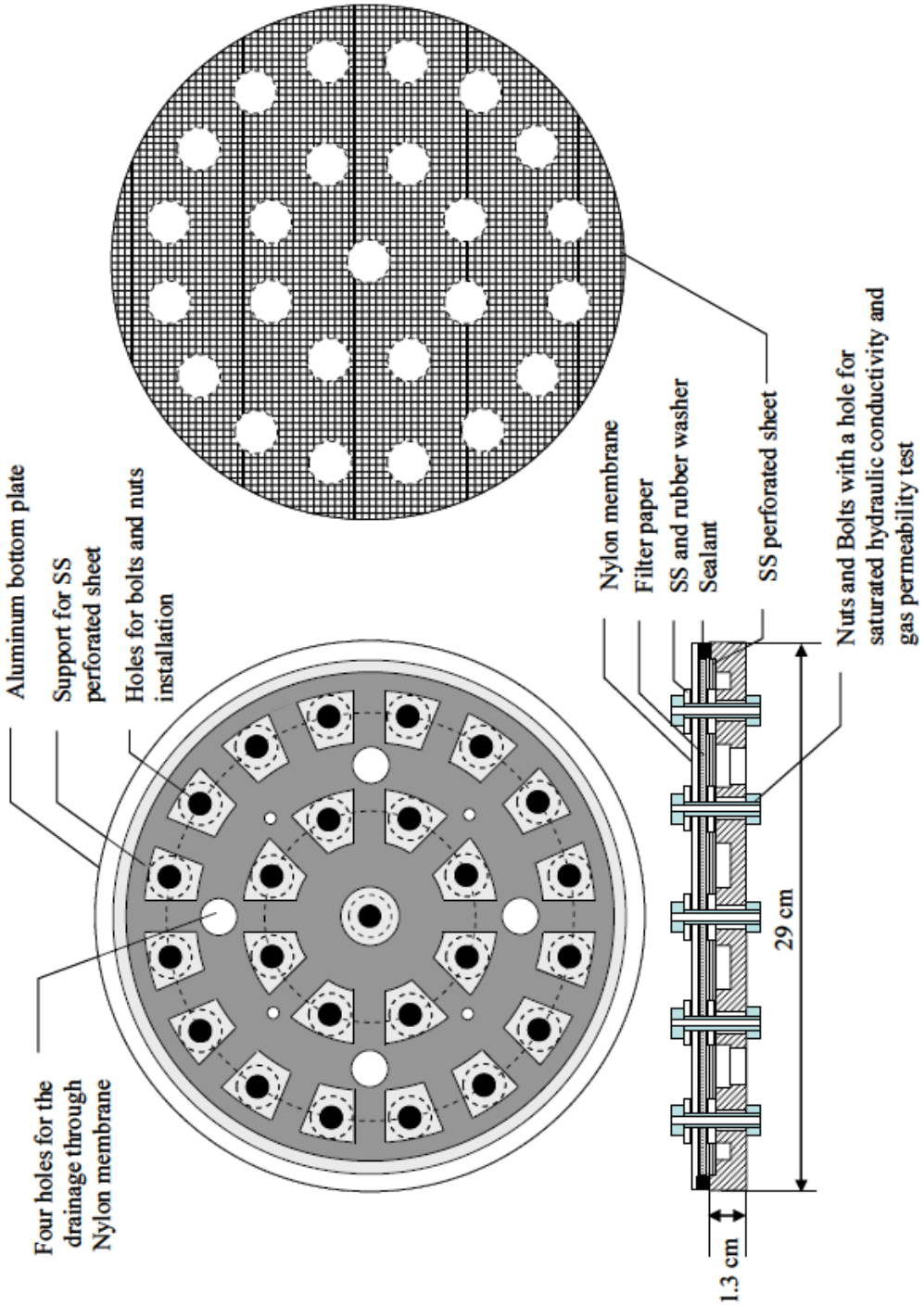

Figure 2.2 Detailed design of the bottom plate used in the newspaper tests (Han, 2009)

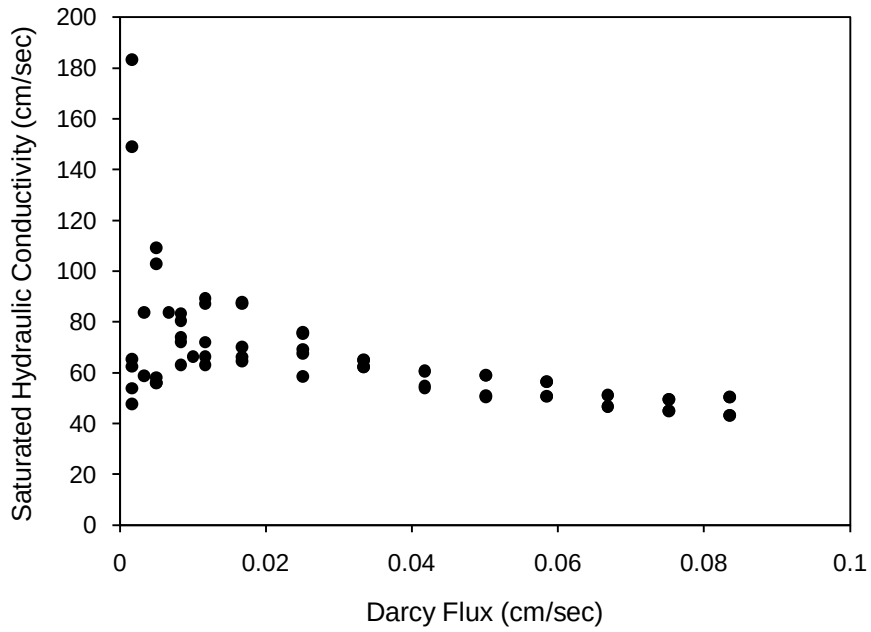

Figure 2.3 The change in saturated hydraulic conductivity with flow rate for column C.

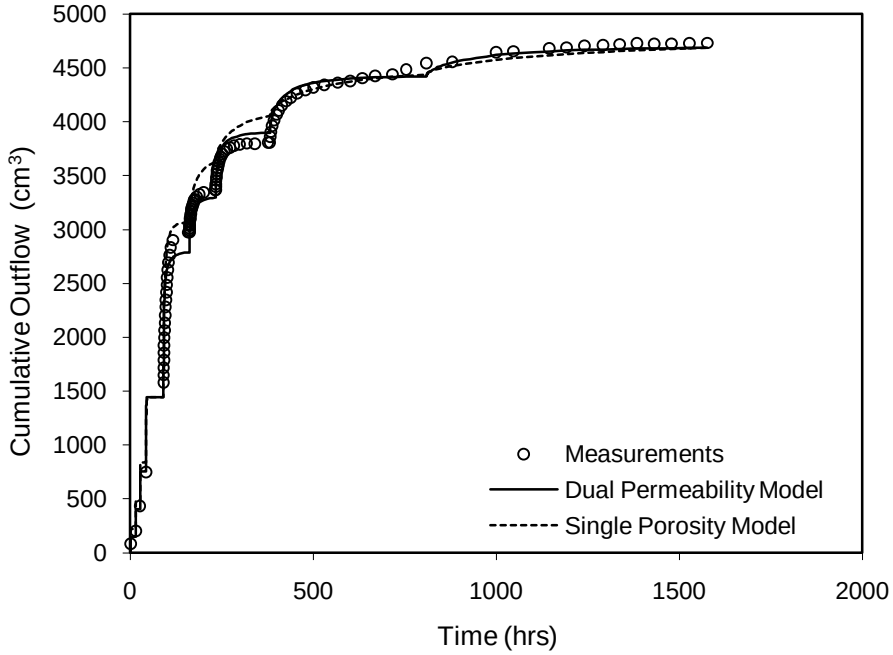

Figure 2.4 Outflow flux data for column C with inverse modeling fits using the best fit parameters from Tables 2.5 and 2.6.

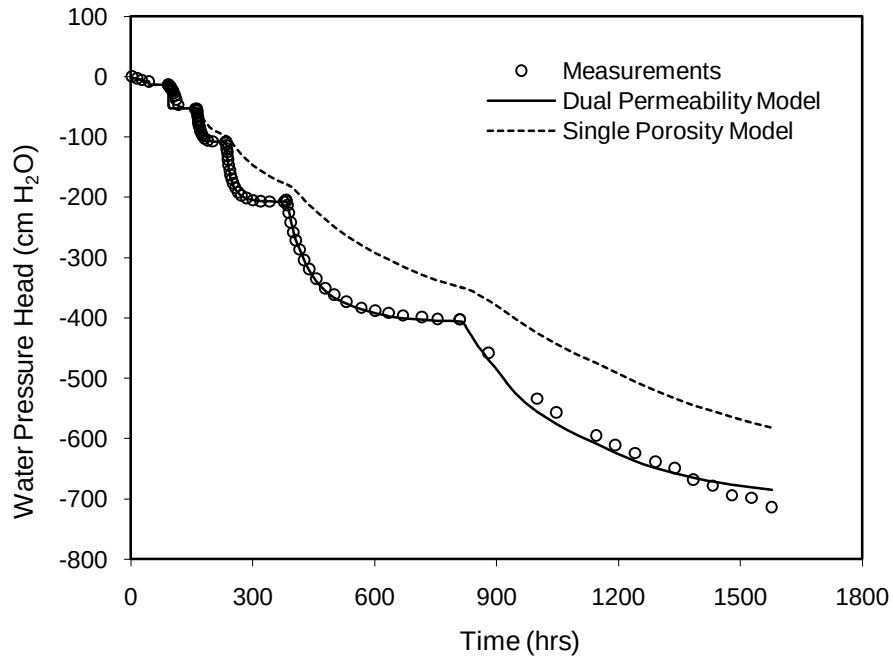

Figure 2.5 Water pressure data for column C with inverse modeling fits using the best fit parameters from Tables 2.5 and 2.6.

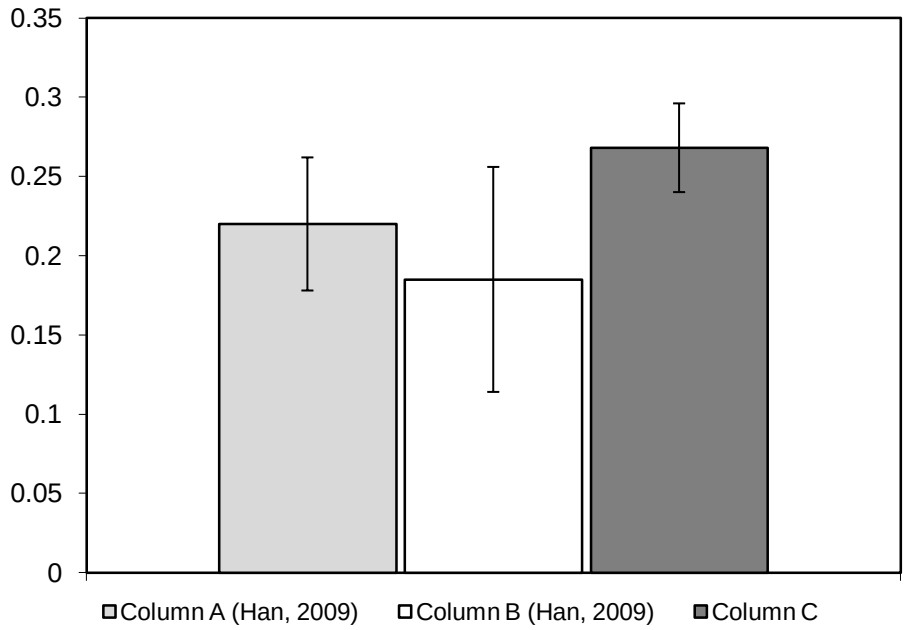

Figure 2.6 Comparison of the fitted residual water content of the matrix domain for columns A, B and C.

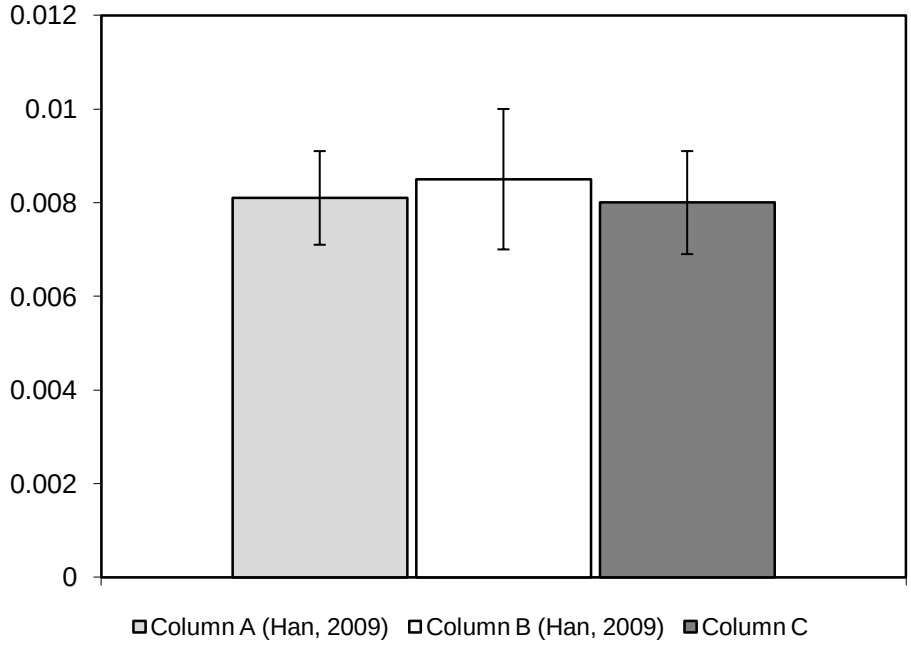

Figure 2.7 Comparison of the fitted alpha value of the matrix domain for columns A, B and C.

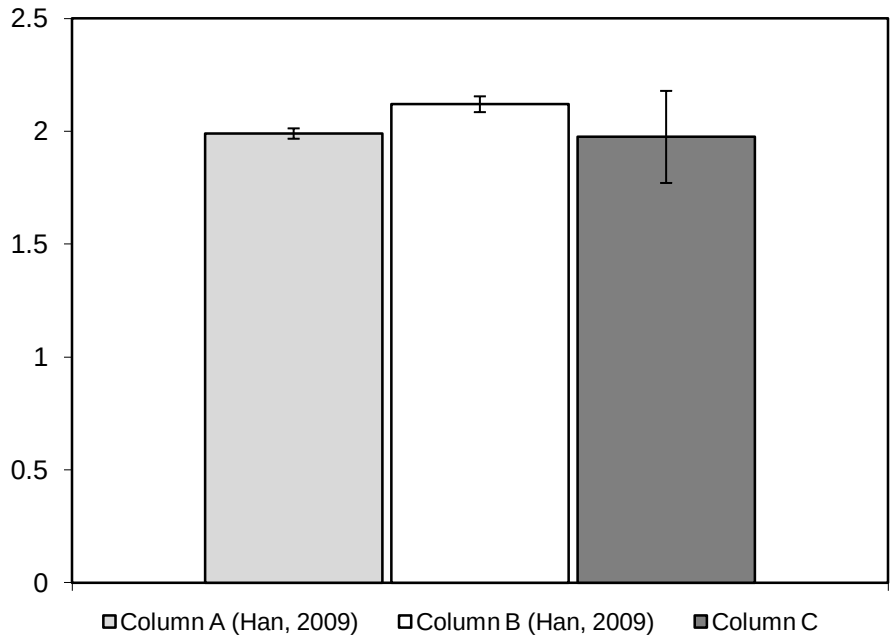

Figure 2.8 Comparison of the fitted n value of the matrix domain for columns A, B and C.

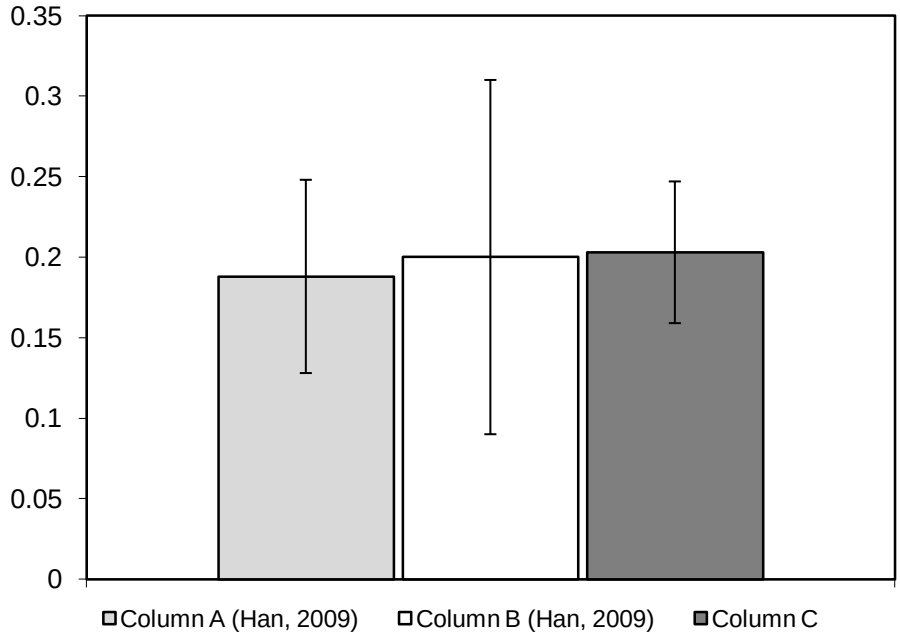

Figure 2.9 Comparison of the fitted saturated hydraulic conductivity value of the matrix domain for columns A, B and C.

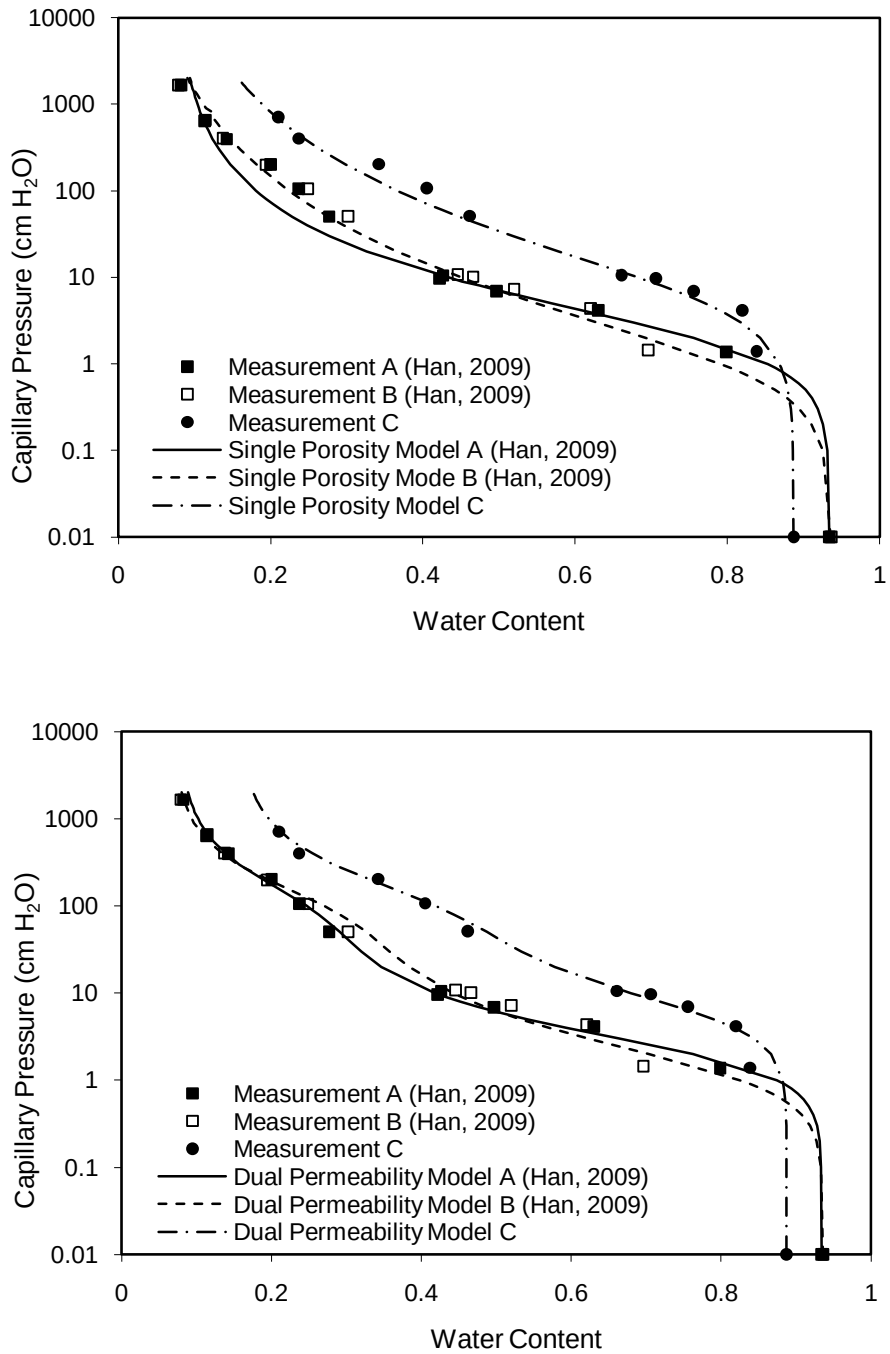

Figure 2.10 The capillary pressure-volumetric water content relationships for columns A, B, and C. The lines show the best fit model predictions for the single porosity (upper plot) and dual permeability (lower plot) models.

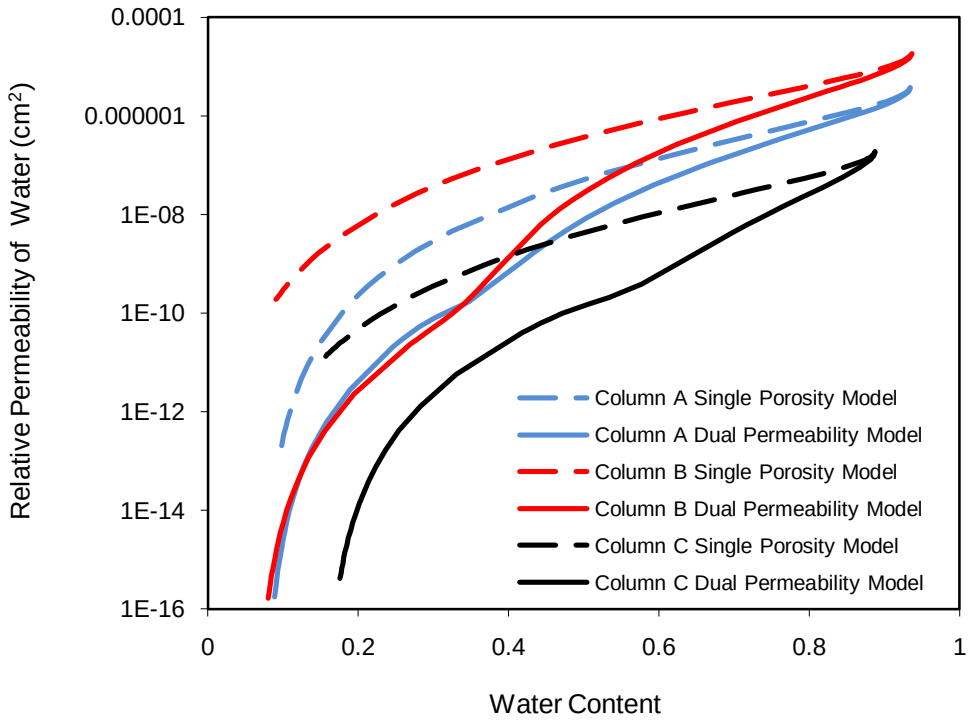

Figure 2.11 Permeability-volumetric water content relationship for Column C.

Chapter 3

COLUMN TESTS ON REAL WASTE SAMPLES

3.1 Background

Based on the previous work from this study and Han (2009) concerning idealized waste samples and the use of a dual permeability model to describe fluid flow through the waste, the next step in testing would be to use real solid waste samples. It would be very useful to be able to determine hydraulic parameters that define the flow of leachate through a landfill. In an attempt to do this, it was hoped that the experiments and procedures from the previous tests on newspaper samples could be applied to real solid waste samples. However, due to the dirty and degradable nature of real waste, problems with clogging the nylon membrane used in the multi step outflow test were encountered.

It was, therefore, necessary to alter the testing methods used to determine the transient water flow data necessary for the inverse modeling. The evaporation method suggested by Wind (1968) is used by many soil scientists (Schwärzel et al., 2006; Ciollaro and Romano, 1995; Šimůnek et al., 1999) as an alternative to the multi step outflow method. However, preliminary attempts to apply the evaporation method to an idealized waste sample of newspaper, in the hopes that the results of the previous multi step outflow tests could be reproduced, were not met with success. Model parameters determined from the multi step outflow test could not accurately describe the water flow observed in the evaporation experiment. It is believed that the high gradients in relative humidity from the bottom to the top of the evaporation column

caused water vapor diffusion through the column which is not accounted for in the HYDRUS-1D modeling procedure. Also, the presence of impervious materials in a sample composed of real waste could cause a loss of hydraulic connectivity between the dry top of the sample and the wetter bottom.

Due to time constraints and the failed evaporation test, it was determined that the best way to proceed would be to use the drainage test as described in Chapter 2 to determine the fracture properties of real waste samples. The data from this test can be analyzed using a single porosity model in two ways. One is to analyze the data the same as in Chapter 2, assuming a single pore domain for the whole sample, but using only data from the drainage test instead of the more extended data set including the multi step outflow data. The other method was to assume that the real waste is best described by a dual domain model and that the properties observed in the drainage test were those of the fracture only. The single porosity model could then be applied to determine the fracture properties of real waste samples.

Four separate real waste samples (RWA, RWB, RWC, and RWD) were tested, each having the same composition. Three of the four tests from the newspaper experiments were performed on the real waste samples; the saturated hydraulic conductivity test, the drainage test, and the porosity test. It was the primary goal of this work to use the drainage test to determine the hydraulic parameters of the fracture domain for real waste samples and to compare those parameters with previous work reported in the literature.

3.2 Materials and Methods

3.2.1 Column design

The column design for the real waste tests was based on the columns used in the newspaper tests by Han (2009) with some modification. The columns were again fabricated from 29 cm inner diameter schedule-80 PVC pipe. Also like the previous column, they were divided into three sections, an upper chamber, a middle chamber for the compressed waste, and a lower chamber. However, where the previous column was all one piece, the column designed for the real waste samples was divided into three separate pieces.

Four middle chambers were made, one to hold each waste sample. The middle chambers consisted of a 2.54 cm thick PVC bottom plate with 25- 2.54 cm diameter holes drilled in it glued to the 29 cm ID PVC pipe. The PVC bottom plate had a stainless steel perforated sheet attached to it with 0.16 cm holes and an open area of approximately 41%. The PVC pipe had two sampling ports on one side where tensiometers could be installed to record the water pressure. There were also eight ports around the top of the PVC pipe where stainless steel rods could be inserted to hold a 1.27 cm thick aluminum top plate in place to keep the sample compressed. One of the 1.27 cm thick aluminum plates was reused from the newspaper test and contained 41 holes (2.54 cm diameter) to allow water to flow through. The other three plates were upgraded to include more holes (0.64 cm diameter) drilled wherever there was space in addition to the 41 larger holes. All of the aluminum plates had a stainless steel perforated sheet (0.16 cm diameter holes, 41% open area) attached to prevent the waste from poking through the larger diameter holes. In this manner, all four of the

middle chambers could be packed with waste at one time and stored in a cold room at 5 °C until ready to be used.

There was only one set of top and bottom chambers made. They were reused for each of the four middle chambers. The top chamber had three testing ports used for saturated hydraulic conductivity testing and draining excess water from the column. The bottom chamber had three ports as well; these used for hydraulic conductivity testing and draining the column during the drainage test. The bottom chamber also contained an aluminum x-brace to increase the structural integrity of the column.

Where two sections of the column came together, there was a ring gasket (aramid/SDR rubber, Part #4459K65, McMaster Carr, Cleveland, OH) between them to ensure an air and watertight seal. The three sections were held together by placing a 1.27 cm thick plate on the bottom and the top and tightening six stainless steel threaded rods connecting the top and bottom. The total height of the assembled pieces was approximately 50 cm. A detailed drawing of the column can be seen in Figure 3.1.

3.2.2 Column preparation

A recent report by the USEPA (2009) listed the generation and recovery of materials for a number of waste categories. The waste categories were paper and paperboard, glass, metals, plastics, rubber and leather, textiles, wood, other materials, food waste, yard trimmings, and miscellaneous inorganic wastes. By subtracting the recovery from the generation, it is possible to calculate the weight of materials discarded, presumably to landfills. From these weights, it is possible to calculate the

percentage of the total weight for each type of material discarded. The results of this are presented in Table 3.1.

The paper category was composed of a combination of newspaper, cardboard, typical printer paper, and glossy paper, such as wrapping paper. The glass portion consisted of broken bottles and jars. The majority of the metal material was aluminum cans, but also included various other metal scraps, including some steel. The plastic category included various types of plastic packaging, such as food and drink containers or cling wrap, as well as more solid plastic, such as the shell of a broken hairdryer. The rubber and leather used for the real waste samples was primarily taken from shoes. Various articles of clothing including blue jeans and cotton shirts were used for the textile portion of the waste. The wood used was old scraps of plywood and boards. The other category was not included in this study. In the USEPA (2009) report, it was mainly composed of used diapers. The food waste was composed of average household food waste. There was a combination of fruit rinds, meat, and animal bones, eggshells, and other common food wastes. Grass, leaves, and dead shrubs made up the yard trimmings portion. The miscellaneous inorganic waste was composed of pieces of brick that were broken to various sizes.

In order to be consistent with the previous tests run on newspaper, it was determined that the real waste cells would be packed to a bulk density of approximately 210 kg/m^3. Because the waste was only air dried at the time it was sorted and packed, the dry densities are lower and are 163, 199, 202, and 199 kg/m^3 for RWA, RWB, RWC, and RWD, respectively. These densities are also consistent with tests done by Chen and Chynoweth (1995) on samples with densities of 160, 320 and 480 kg/m^3.

Knowing the approximate volume of the real waste cells, the desired packing density, and the percentages of discarded waste from the USEPA (2009) report, it was possible to determine the weight of each material to be put in each column. Instead of digging waste out of a landfill, it was decided that waste would be collected over a period of approximately one week from a household in Lancaster, Pennsylvania and then sorted and divided up by hand into the proper proportions.

Once all of the waste was collected and sorted, any large pieces were cut to a more manageable size so they would fit into the columns with the largest particles being no bigger than approximately 15 cm in the longest dimension. Due to the small size of the columns relative to the waste, the majority of the waste was cut to some degree. Some pieces were cut small and some were left larger. After sorting and cutting, the air dried material from each waste category was weighed to the proper amount and then poured into a plastic bag. In an attempt to keep all four samples as similar as possible, during the sorting process an equal number of small, medium and large particles of each material were handpicked used in each cell. The compositions of each cell can be seen in Table 3.2.

Once the waste was divided into four bags (one for each compression cell), it was packed into the cells using a hydraulic compressor. Before adding the waste, it was shaken up in a plastic container and mixed thoroughly by hand. It was then added a bit at a time until all of the waste had been packed. Once all of the waste was in the columns, the eight stainless steel support rods were inserted into the sides of the compression cells to hold the aluminum top plate down. The final height of the waste samples was approximately 9 cm for RWB, RWC and RWD. The column for RWA had been constructed at an earlier time, and was, therefore, slightly longer than

the other columns which resulted in a height of 10.6 cm for RWA. This column also used the aluminum top plate with fewer holes as discussed above. Table 3.3 shows the packing properties for the four real waste columns.

Once the columns were packed, the ceramic cup tensiometers were installed and the column was saturated as previously described in Chapter 2, changing the degassed water injection to 0.22 L/min for one hour and thirty minutes to account for the somewhat smaller column.

3.2.3 Saturated hydraulic conductivity test

The saturated hydraulic conductivity test was performed in the same manner as previously stated in Chapter 2 with two small deviations. The saturated hydraulic conductivity test for the real waste samples was performed before the drainage test to save time. Also, whereas pressure gradient measurements were previously taken between a point in the waste sample and the top chamber, measurements for the real waste samples were taken at these same positions as well as from the top chamber to the bottom chamber (a longer distance) due to very low gradients from the shorter distance.

3.2.4 Drainage tests

The drainage tests for the real waste samples followed the same general procedure as described for the newspaper samples in Chapter 2. However, for RWB, RWC, and RWD there are some key differences. The first column, RWA, was allowed to run using the same procedure as had been used before. However, preliminary analysis of the data was unclear as to whether the outflow lines and connections were limiting the rate at which the water was flowing out of the column.

To ensure that the tubing would not affect the rate data, it was determined that three outflow tubes and smaller incremental step sizes should be used.

In order to control the outflow from three tubes, it was necessary to build a manifold that would accommodate all of the outflow. The design chosen was to use a clear, 2.54 cm diameter PVC pipe with a corresponding 2.54 cm diameter PVC valve in the middle. The three outflow tubes coming from the column would all flow into the PVC manifold, through the valve, and then out through three shorter outflow tubes. A sketch of the manifold can be seen in Figure 3.2. This set up made it possible for one person to start and stop the outflow at the beginning and end of each step. This procedure was followed for tests RWB, RWC, and RWD.

The other modification to the original procedure was to reduce the step size. The RWA test had been run with four steps, each draining a height of 2.66 cm. It was determined that the smallest possible step to take without incurring large experimental errors would be 1 cm. Therefore, tests RWB, RWC, and RWD were run using nine steps, each draining a height of 1 cm. This reduction in height brought about a reduction in flow velocity, which allowed for more accurate measurement of the rate data. Table 3.4 shows the bottom boundary conditions for the four experiments.

3.2.5 Porosity test

The porosity test was performed using the same procedure as described in Chapter 2 except that there was no M0 step. The volume of water drained from the column was only the water drained by gravity without any applied gas pressure. Also, in the case of the real waste samples, a separate drainage test was not performed. Since there was no multi step outflow test for these samples, after the drainage test

was finished, the samples were removed and dried in the oven instead of re-saturating the samples and performing another drainage test.

3.3 Results

3.3.1 Saturated hydraulic conductivity and porosity

As seen in Chapter 2, when calculating the saturated hydraulic conductivity, it is first necessary to determine whether or not Darcy's law applies. Again, Equation 2.1 suggested by Seguin et al., (1998) is used to determine the pore Reynolds number. The samples used in the real waste tests are irregular in shape. However, most could be estimated as roughly spherical or plate shaped. Seguin et al., (1998) conducted research using beds packed either with spherical or plate particles and found a number of different limits for the end of laminar flow. The lowest of these limits, for parallel plates is 80. While the samples in this study are not strictly on shape, using the lowest limit of 80 should be a safe assumption. Using Equation 2.1 with the longest characteristic length of any particle in the sample, d = 15, the pore Reynolds number that corresponds to a Darcy flux of 0.017 cm/sec is Re_{pore} = 58, which is low enough to be considered laminar. This holds true for all of the real waste columns. The saturated hydraulic conductivity can be seen plotted against the Darcy flux in Figure 3.3.

The saturated hydraulic conductivities calculated for the real waste samples are 2.4 x 10^{-2}, 1.3 x 10^{-2}, 6.2 x 10^{-3}, and 1.7 x 10^{-2} m/s for RWA, RWB, RWC, and RWD, respectively. It is interesting to note that although the samples were very similar in composition, the saturated hydraulic conductivities have a range from 10^{-2} to 10^{-3} m/s. When compared to other values in the literature, the hydraulic

conductivities found in this study are slightly high. The literature values for both field and laboratory testing cover a range from 10^{-3} to 10^{-9} m/s with most of the values in the range of 10^{-4} to 10^{-6} m/s based on various studies (Beaven, 2000).

However, it is important to note that almost all of the work in the literature was performed at higher compaction densities than the tests performed in this study. A number of papers have shown that as densities and applied stresses increase, the hydraulic conductivity decreases (Beaven, 2000). Two laboratory tests from Beaven's review have densities near what was used in the study presented here (Fungaroli and Steiner, 1979; Chen and Chynoweth, 1995). Fungaroli and Steiner (1979) used samples with densities ranging from less than 100 kg/m^3 to 350 kg/m^3 and found corresponding conductivities ranging from 1 x 10^{-4} to 1 x 10^{-6} m/s. Chen and Chynoweth (1995) used densities of 160, 320, and 480 kg/m^3 and found conductivities in the range of 9.5 x 10^{-4} to 5 x 10^{-7} m/s. The saturated hydraulic conductivity values for this study and others can be seen in Table 3.5.

As stated before, one possible reason for the low conductivity values obtained in these tests could be the lower dry density used. This lower density was used in order to be consistent with the previous set of tests that were performed on the idealized newspaper sample and also because it was feared that the PVC bottom plates which were glued to the PVC pipe in the compression cells might fail if more load was applied during the packing process. Another possible reason for the difference in saturated hydraulic conductivities could be the presence of entrapped air, which would cause a lower conductivity. When samples were saturated, they were first purged with CO_2 gas, which has a higher solubility in water than air. A vacuum was then applied to remove all gas before degassed water was injected. Using this procedure, there is a

high probability that the majority of the sample was saturated without entrapped air. The procedures used to saturate the samples in the three previously mentioned studies were not as rigorous and, therefore, could have allowed the entrapment of air in the samples. This would account for the reduced values for the saturated hydraulic conductivity.

The total porosities calculated for the real waste tests were ε = 0.829, 0.823, 0.769, and 0.821 for RWA, RWB, RWC and RWD, respectively. These values initially look much higher than values found in the literature as reviewed by Beaven (2000) which are typically 0.3 to 0.5 for laboratory testing and 0.03 to 0.16 for field testing. However, these values from the literature are reported as specific yields, or effective porosities as calculated in Equation 3.1.

$$\varepsilon_e = \frac{V_{w-d}}{V_T} \tag{3.1}$$

where ε_e is the effective porosity, $V_{w\text{-}d}$ is the volume of water which drains freely under the influence of gravity, and V_T is the total sample volume (Beaven, 2000). Using Equation 3.1, the effective porosity values for the real waste tests conducted in this study become ε_e = 0.526, 0.531, 0.453, 0.520 for RWA, RWB, RWC and RWD, respectively. These values are still at the high end of the range reported in the literature, but are much closer.

Again, a possible explanation for why the values are higher than the literature could be the low densities used in this study. A higher compaction density would result in less volume in the large fractures, and, therefore, lower total and effective porosities. Another reason might be the absence of fines in the samples used in this study. Smaller particles, such as might be introduced in a daily cover, would theoretically fill the larger fractures and reduce the porosity. It is unclear as to why

the effective porosities of laboratory tests appear to be much higher than those of field tests. A comparison of the various porosities can be seen in Table 3.5.

3.3.2 Drainage

Once the data for the drainage tests was collected, they were analyzed in much the same fashion as in Chapter 2. The water pressure and outflow data were divided into 21 evenly spaced data points for each step. The water pressure and outflow data were again converted to capillary pressures and outflow fluxes and the data was inversely modeled using HYDRUS-1D. The modeling was carried out using two different assumptions: that the sample as a whole was composed of a single pore system; or that the sample could be considered a dual domain system and only the fracture domain was tested with the drainage tests. Instead of only using the final data point for the drainage tests, as was done in the previous newspaper study, all data points were used in the inverse modeling process. As stated before, it was unclear based on preliminary analysis of the data as to whether or not the tubing and connections affected the rate of outflow for the first test, RWA. To determine whether the data could be used, one outflow step with the same height, but no waste was drained. The data from this step without waste was compared to the data with waste. It could be seen that the water coming from the step with waste flowed more slowly. Therefore, the outflow rate was controlled by the waste sample and not the tubing and connections. After this further investigation, it was determined that all data points could be used.

3.3.2.1 Single porosity modeling

For the first modeling process, it was assumed that the real waste samples were made up of a single pore domain and could, therefore, be modeled using the same single porosity model used in Chapter 2. The saturated hydraulic conductivity (K_s) and saturated water content (θ_{ws}) were measured independently and the tortuosity parameter (l) was assumed to be 0.5. This again left the residual water content (θ_{wr}), and the van Genuchten parameters (α and n) to be fitted by HYDRUS-1D. The fitted parameters obtained from HYDRUS-1D can be seen in Table 3.6 and the model fits can be seen in Figures 3.4 and 3.5. Although two tensiometer locations were used in the experiments and modeling, the fits are only shown for one tensiometer so as not to show multiple graphs which demonstrate the same model fits.

There are relatively few measurements of the hydraulic parameters of real waste samples. A short review of the few that are available was presented by Zardava et al. (2009). Zardava et al. (2009) report on findings from Kazimoglu et al. (2006) and Mansoor (2003). Kazimoglu et al. (2005) found θ_{wr} = 0.14, α = 0.014 and n = 1.6 for a synthetic solid waste based on a landfill site in Lydhurs, Australia. Mansoor (2003) reported values of θ_{wr} = 0.01, α = 0.0049 and n = 1.45 based on the use of the filter paper method on a synthetic waste with a dry density of 350 kg/m^3. These values, as well as those determined in this study, can be compared in Table 3.7. The values for all three parameters determined from these three studies cover a wide range; from 0.01 to 0.187 for θ_{wr}, from 0.0049 to 2.17 for α, and from 1.45 to 2.72 for n. Based on these observations, it might be very difficult to determine a uniform set of parameters that describe fluid flow for solid waste.

3.3.2.2 Fracture domain modeling

The second assumption made when modeling the data from the real waste drainage tests was that the waste can be described as a dual domain system. If this is the case, which seems likely based on preferential flow patterns as discussed previously, a much larger set of parameters is required to accurately describe fluid flow through a landfill. Using the assumption that the drainage test only represents flow out of the fractures, the van Genuchten parameters for the fracture domain (α_f and n_f) can be determined.

First, it must be assumed that all of the water has been removed from the fractures at the end of last drainage step. This assumption allows θ_{wr} to be set to zero. As previously assumed in Chapter 2, since the fractures are large and there are no fine particles in the waste, θ_{ws} can be set equal to one. Using the independently measured hydraulic conductivity, $l = 0.5$, and the assumptions above, inverse modeling can be carried out with only the van Genuchten parameters for the fracture domain to be fitted. Because the outflow is considered to only come from the fractures, the outflow flux used in the HYDRUS-1D modeling must be divided by the ratio of fracture volume to the total volume of the sample, w_f. In order to calculate w_f, it was assumed that the volume of water that flowed out at the end of the drainage test was equal to the volume of fractures in the sample. This volume was then divided by the total volume of the sample to obtain w_f. To the best of our knowledge, this is the first attempt to determine any parameters that assume a dual permeability model for solid waste. The fitted parameters and best fits for the data can be seen in Table 3.8 and Figures 3.6 and 3.7, respectively.

3.3.3 Capillary pressure – volumetric water content – permeability relationship

Using the same methods as in Chapter 2, the capillary pressure-volumetric water content relationship was predicted using the parameters from the single porosity model for each of the four waste samples. Figure 3.8 shows the data and the model predictions for the capillary pressure-volumetric water content curves for the four solid waste samples examined in this study.

For reference, the four capillary pressure-volumetric water content curves from this study are plotted along with curves calculated using the model parameters from Kazimoglu et al. (2006) and Mansoor (2003) in Figure 3.9. It is clear that the relationships are not all the same. There is some variation even among the four samples analyzed in this study, which had very similar compositions and densities. All four curves have a similar slope in the range $0.4 \leq \theta_w \leq 0.65$, but where RWA, RWB and RWD have similar values for θ_{wr} and θ_{ws}, RWC has slightly different values. The variability that can exist in real waste is probably illustrated best by the pressure-saturation relationships for the different waste samples shown in Figure 3.9.

The permeability-volumetric water content curves calculated from the single porosity mode for the four real waste samples can be seen in Figure 3.10. It is interesting to see that the curves for RWA and RWC are similar and the curves for RWB and RWD are similar, but the two pairs differ quite a bit from each other.

3.4 Validation of porosity testing methods

Due to the high porosities observed in the real waste samples from this study, it was decided that the testing methods used to determine the porosities should be verified. In order to verify that the method used was measuring the porosity correctly, it was necessary to use a medium for which the porosity could be

determined both experimentally and theoretically. Four hundred and forty plastic balls (2.54 cm diameter) were packed in one of the test columns (28.8 cm diameter) to a height of 10.5 cm. A single step drainage test was run on the sample with the outflow volume used to determine the volume of the voids experimentally.

The porosity can be calculated theoretically using the geometry of the column, the geometry of the balls, and the number of balls. Since the number of balls and the diameter of the balls is known, the total volume occupied by the balls in the column could be calculated (V_s = 3775.3 cm^3). The total volume of the column was calculated using the diameter and height of the column (V_T = 6840.1 cm^3). Therefore, the theoretical porosity of the sample can be calculated by subtracting the volume of the balls from the total volume to get the volume of the voids and dividing by the total volume (ε_T = 0.4481).

Experimentally, the total volume of water that was drained from the column during the drainage test (V_d = 3048.2 cm^3) represents the volume of the void space in the column. Dividing the volume of the voids by the total volume then yields the measured porosity (ε_M = 0.4456). As can be seen from the very close theoretical and measured values for the porosity of the sample, the method used to determine the porosity of the samples composed of real waste is valid and produced the correct results. However, as the porosities are much higher than those found in the literature, it is necessary to do more testing to determine a definite cause for the discrepancy.

3.5 Summary and Conclusions

Three of the four tests which were previously used only for idealized waste samples composed of newspaper were modified and applied to four samples composed of real waste materials which are representative of those found in a landfill.

The objective of these tests was to develop constitutive relationships for real waste samples and compare the findings with similar tests that have been run by other researchers. Two different methods were used to model the data obtained from the solid waste experiments. One method assumed a single pore domain and the results of these models can be directly compared to similar results in the literature. The other method assumes a dual domain system. To the best of our knowledge, the information about the fracture domain resulting from this second assumption has never been investigated. The results should provide a good starting point for better understanding and describing the flow of liquids in a landfill using a dual permeability model.

The results obtained from testing four samples made up of real waste materials show that even when the composition and densities of the samples are very similar, some variability can be seen in the hydraulic properties of the waste. When the results of this test were further compared with results found in the literature based on samples with different compositions and compaction densities, it was clear that the variability in the hydraulic properties becomes even more pronounced.

Table 3.1 Waste generation, recovery and disposal based on the USEPA (2009) study in millions of tons (assumed to be air dried)

Material	Waste Generated	Waste Recovered	Waste Discarded	Percent Discarded
Paper	77.42	42.94	34.48	21.1%
Glass	12.15	2.81	9.34	5.7%
Total Metals	20.85	7.22	13.63	8.3%
Plastics	30.05	2.12	27.93	17.1%
Rubber and leather	7.41	1.06	6.35	3.9%
Textiles	12.37	1.89	10.48	6.4%
Wood	16.39	1.58	14.81	9.1%
Other[1]	4.5	1.15	3.35	0.0%
Food	31.79	0.8	30.99	19.0%
Yard trimmings	32.9	21.3	11.6	7.1%
Misc. inorganic waste	3.78	0	3.78	2.3%
Total	**249.61**	**82.87**	**166.74**	**100.0%**

[1]The Other category was not included in this study, as it was only 2% of the total discarded waste and mainly comprised of used diapers, which were not readily available.

Table 3.2 Waste composition for RWA, RWB, RWC and RWD (weights are air dried)

Material	Weight (g)			
	RWA	RWB	RWC	RWD
Paper	301.7	302.6	302.2	302.2
Glass	82.2	81.6	81.5	82.5
Metal	118.9	118.9	118.7	118.8
Plastic	244	243.6	244.1	243.7
Rubber/leather	55.7	55.8	55.9	56.1
Textiles	91.8	91.8	92.3	91.3
Wood	130.1	129.8	130.5	130.3
Food	271.8	271.6	270.9	271.8
Yard	101.3	100.9	101.2	101.6
Misc. inorganic waste	33.6	33.3	33.5	33.1
Total	1129.4	1127.3	1128.6	1129.2

Table 3.3 Packing properties for the four samples that were tested

	RWA	RWB	RWC	RWD
Diameter of column (cm)	28.8	28.8	28.8	28.8
Height of sample (cm)	10.6	9.1	9.0	9.1
Tensiometer installation[1]	1.9 cm 6.0 cm	2.3 cm 6.0 cm	2.4 cm 5.8 cm	2.5 cm 5.8 cm
Dry weight of waste (g)	1123.5	1186.6	1176.2	1184.4
Packing density (kg/m^3)	163	200	201	200
[1] Measured from the bottom of the sample up to the tensiometer location				

Table 3.4 The water pressure heads for pressure steps at the bottom boundary for RWA, RWB, RWC, and RWD. "G" indicates gravity drainage.

Steps	G1	G2	G3	G4	G5	G6	G7	G8	G9
RWA (cm H_2O)	8.0	5.3	2.7	0	-	-	-	-	-
RWB (cm H_2O)	8.1	7.1	6.1	5.1	4.0	3.0	2.0	1.0	0
RWC (cm H_2O)	8.0	7.0	6.0	5.0	4.0	3.0	2.0	1.0	0
RWD (cm H_2O)	8.1	7.1	6.1	5.1	4.0	3.0	2.0	1.0	0

Table 3.5 Hydraulic conductivity and effective porosity results from this study on real waste and literature values for other waste samples

Author	Hydraulic conductivity (m/s)	Effective Porosity/ Specific Yield	Total Porosity	Dry Density (kg/m3)
Scicchitano (2010)	6.2×10^{-3} to 2.4×10^{-2}	0.45 - 0.53	0.769 – 0.829	210
Chen and Chynoweth (1995)	4.7×10^{-7} to 9.6×10^{-4}	-	-	160 to 480
Fungaroli and Steiner (1979)	1×10^{-6} to 1×10^{-4}	-	-	100 to 350
Oweis et al. (1990)	1×10^{-5} to 1.5×10^{-6}	0.05 – 0.10	0.4 – 0.5	-
Burrows et al. (1997)	3.9×10^{-7} to 6.7×10^{-5}	0.09 – 0.16	-	-
Korfiatis et al. (1984)	8×10^{-5} to 1.3×10^{-4}	0.2 – 0.3	0.5 – 0.6	616
Bleiker et al. (1993)	5×10^{-9} to 1×10^{-6}	-	0.50 – 0.85	500 to 1200
Beaven and Powrie (1995)	1.7×10^{-4} to 2.0×10^{-4}	0.28 – 0.34	-	190 – 440
Mansoor (2003)	-	-	0.35*	350
Kazimoglu (2006)	5.0×10^{-4} (Fitted)	-	0.58*	-

* The reported values are estimated from moisture retention curves.

Table 3.6 Hydraulic parameters optimized with the HYDRUS-1D single porosity model for the real waste samples (± values show the 95% confidence interval)

	θ_{wr} [-]	θ_{ws} [-]	α [cm^{-1}]	n [-]	K_s [cm/hr]	l [-]	R^2
RWA	0.187 ± 0.039	0.8295	1.521 ± 1.057	2.718 ± 0.959	8700.1	0.5	0.952
RWB	0.016 ± 0.015	0.8233	0.939 ± 0.579	1.732 ± 0.110	4526.1	0.5	0.979
RWC	0.167 ± 0.059	0.7688	1.085 ± 0.686	1.966 ± 0.177	2228.5	0.5	0.968
RWD	0.010 ± 0.0003	0.8214	2.175 ± 0.106	1.641 ± 0.037	5971.3	0.5	0.984

Table 3.7 Comparison of hydraulic parameters from the literature with those found in this study

Author	θ_{wr}	α (cm^{-1})	n
Scicchitano (2010)	0.01 – 0.187	0.94 – 2.18	1.64 – 2.72
Mansoor (2003)	0.01	0.0049	1.45
Kazimoglu (2006)	0.14	0.014	1.6

Table 3.8 Hydraulic parameters of the fracture domain optimized with the HYDRUS-1D single porosity model for the real waste samples (± values show the 95% confidence interval)

	θ_{wrf} [-]	θ_{wsf} [-]	α_f [cm^{-1}]	n_f [-]	K_{sf} [cm/hr]	l_f [-]	R^2
RWA	0	1	2.927 ± 1.82	2.762 ± 1.54	8700.1	0.5	0.946
RWB	0	1	1.250 ± 0.483	4.24 ± 0.789	4526.1	0.5	0.962
RWC	0	1	2.819 ± 0.918	3.131 ± 1.419	2228.5	0.5	0.950
RWD	0	1	3.684 ± 0.074	3.196 ± 0.433	5971.3	0.5	0.968

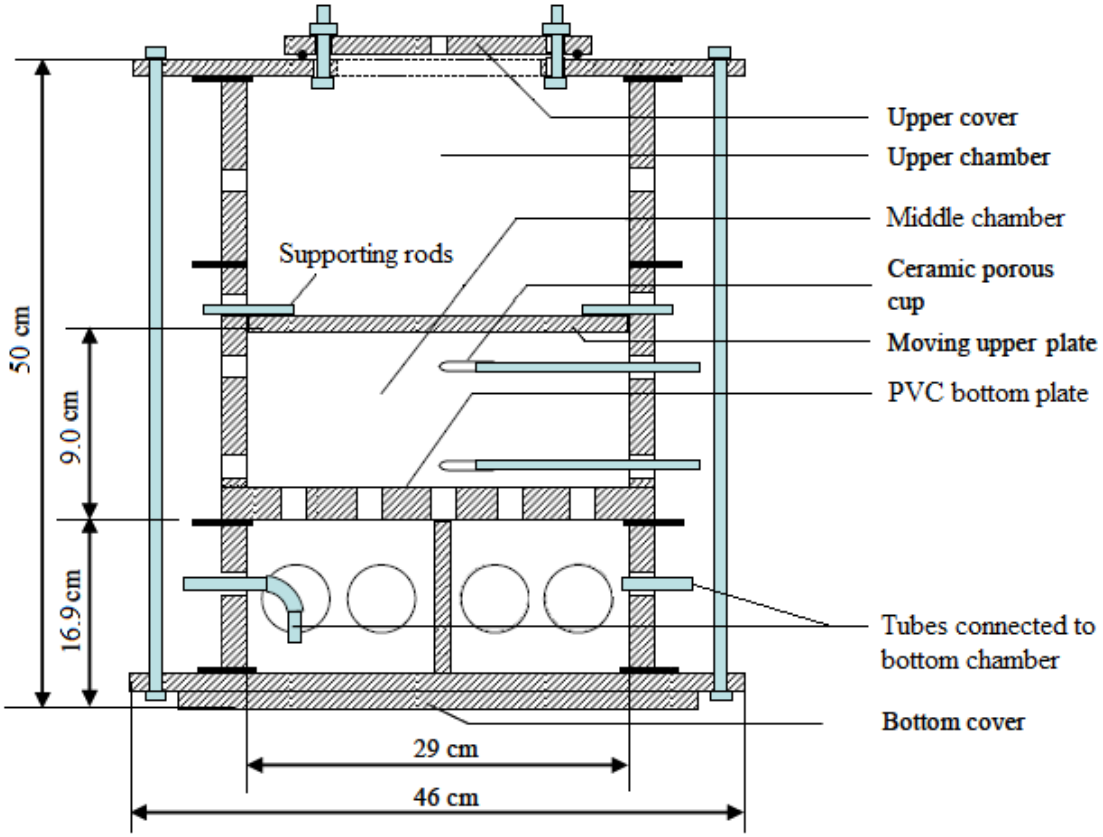

Figure 3.1 Diagram of the experimental columns used in the real waste tests

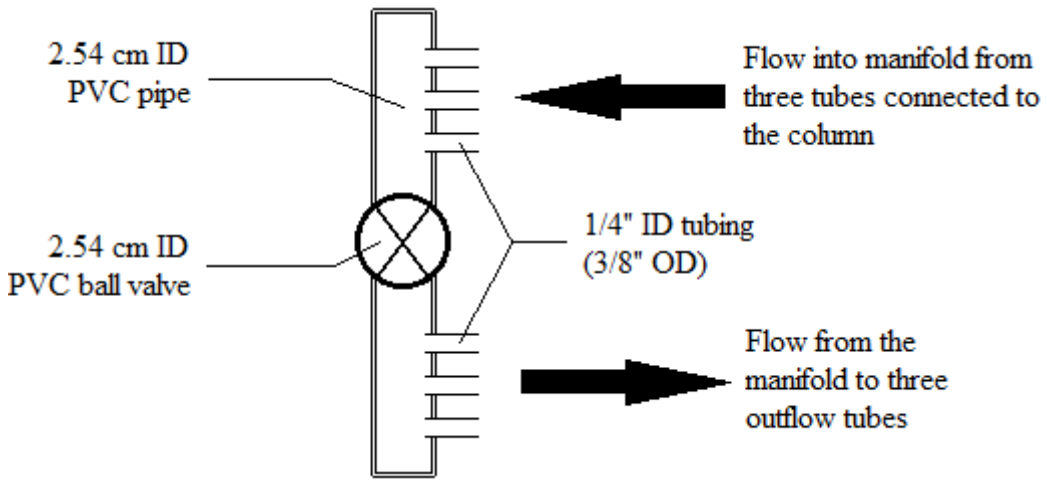

Figure 3.2 Diagram of the manifold used to convey outflow in the real waste tests.

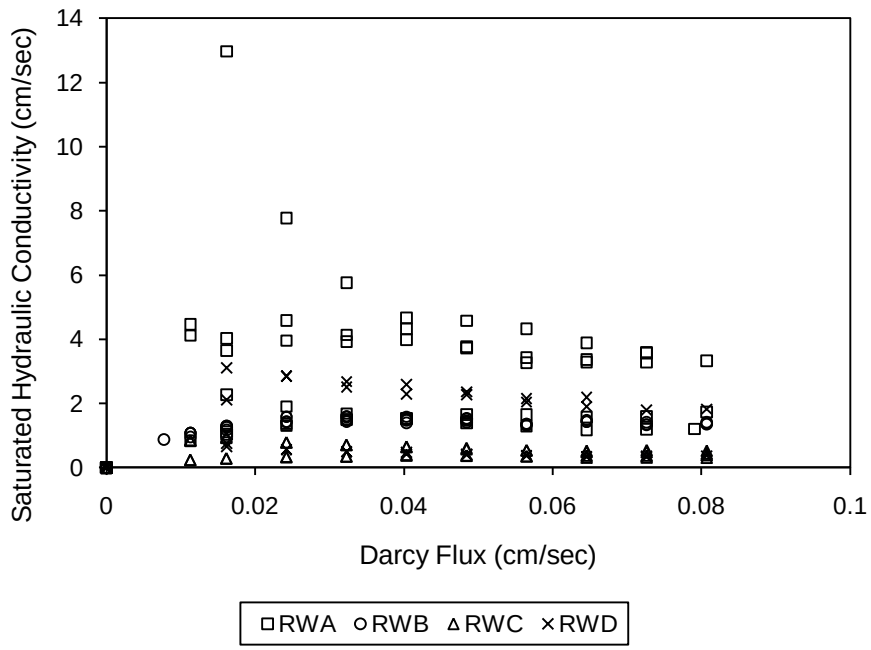

Figure 3.3 The change in saturated hydraulic conductivity with flow rate for the real waste columns

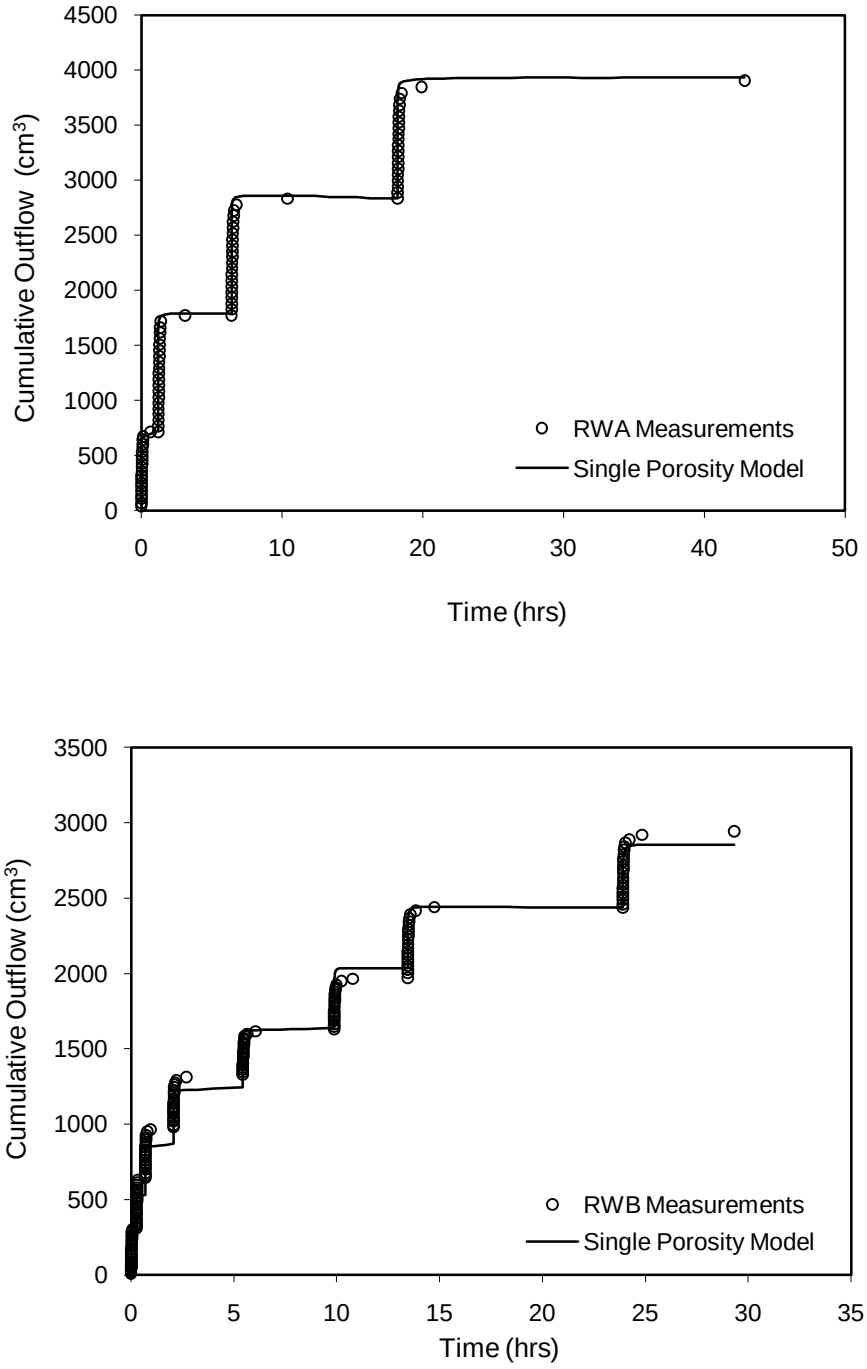

Figure 3.4 Outflow flux data for RWA (upper plot) and RWB (lower plot) with inverse modeling fits using the best fit parameters from Table 3.6. (Figure 3.3 continued on the following page)

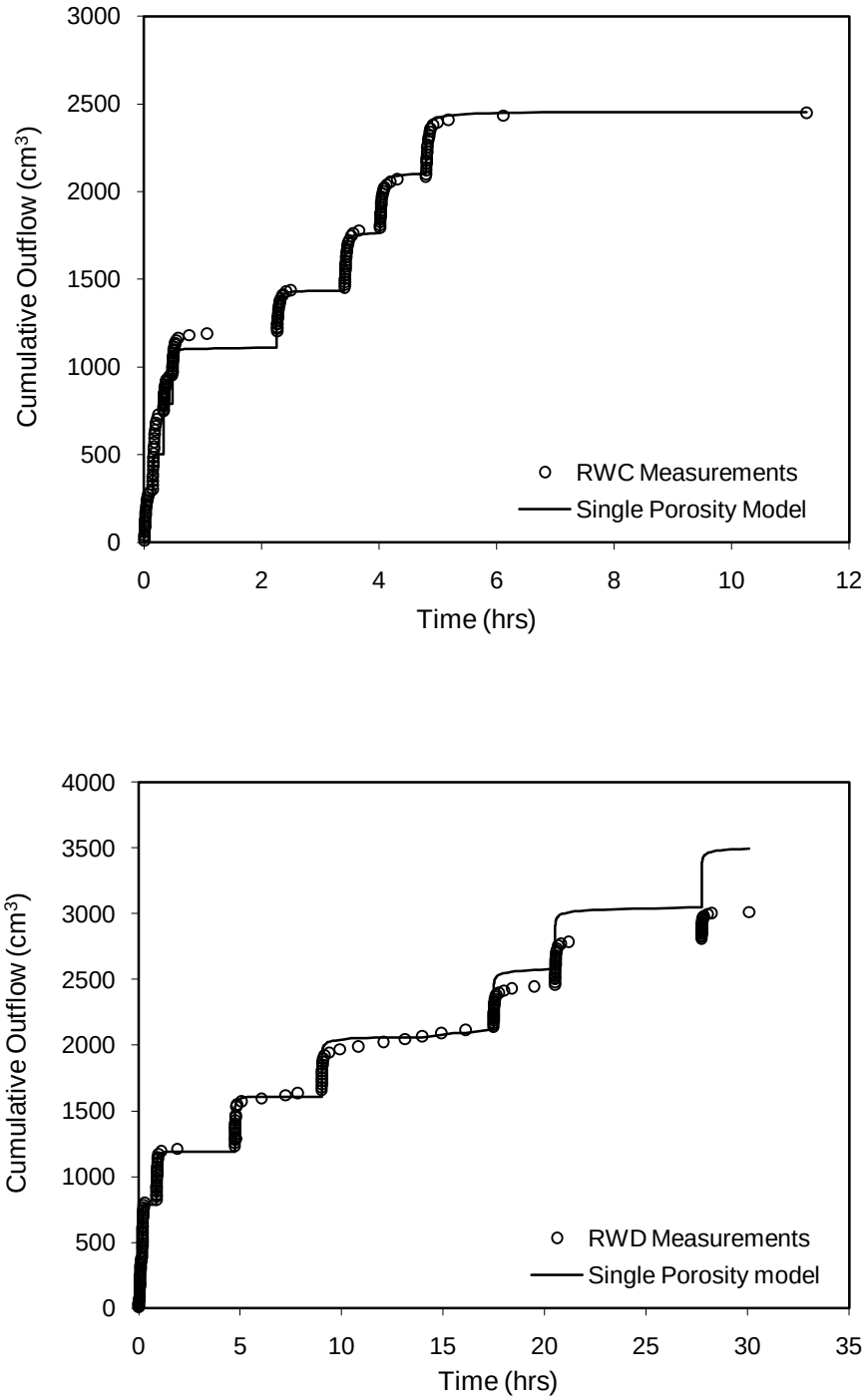

Figure 3.4 Outflow flux data for RWC (upper plot) and RWD (lower plot) with inverse modeling fits using the best fit parameters from Table 3.6

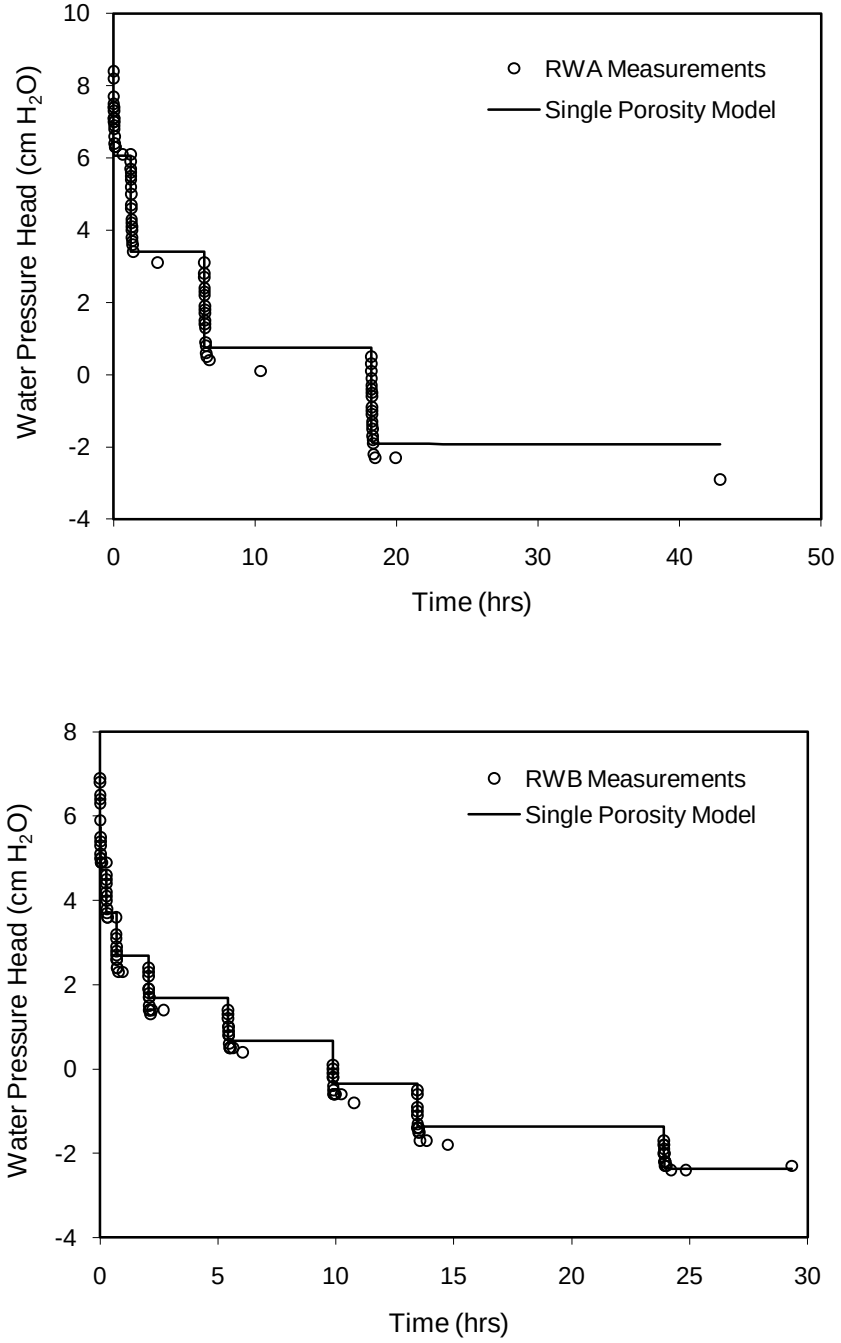

Figure 3.5 Water pressure data for RWA (upper plot) and RWB (lower plot) with inverse modeling fits using the best fit parameters from Table 3.6 (Figure 3.4 continued on the following page)

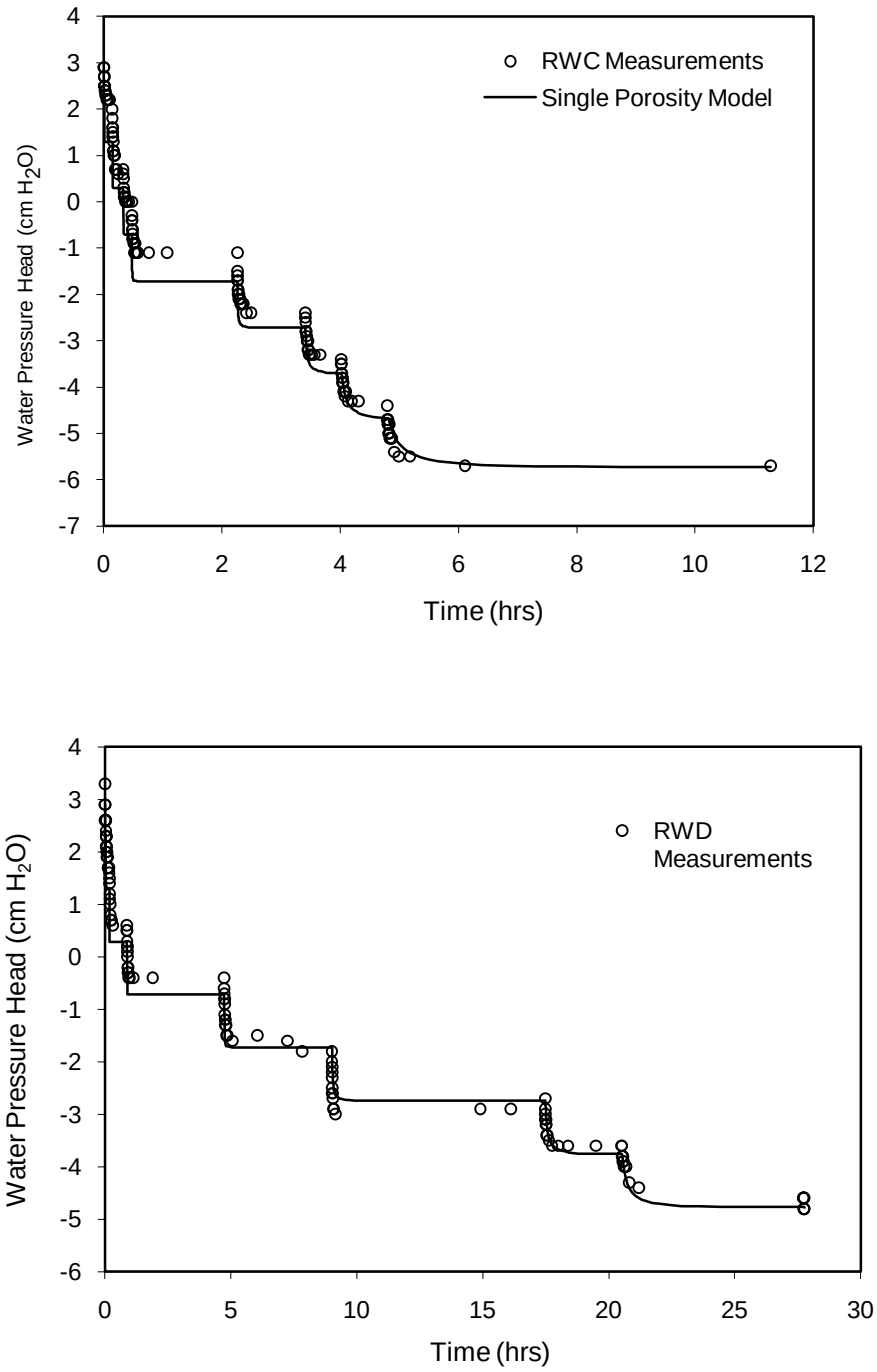

Figure 3.5 Water pressure data for RWC (upper plot) and RWD (lower plot) with inverse modeling fits using the best fit parameters from Table 3.6

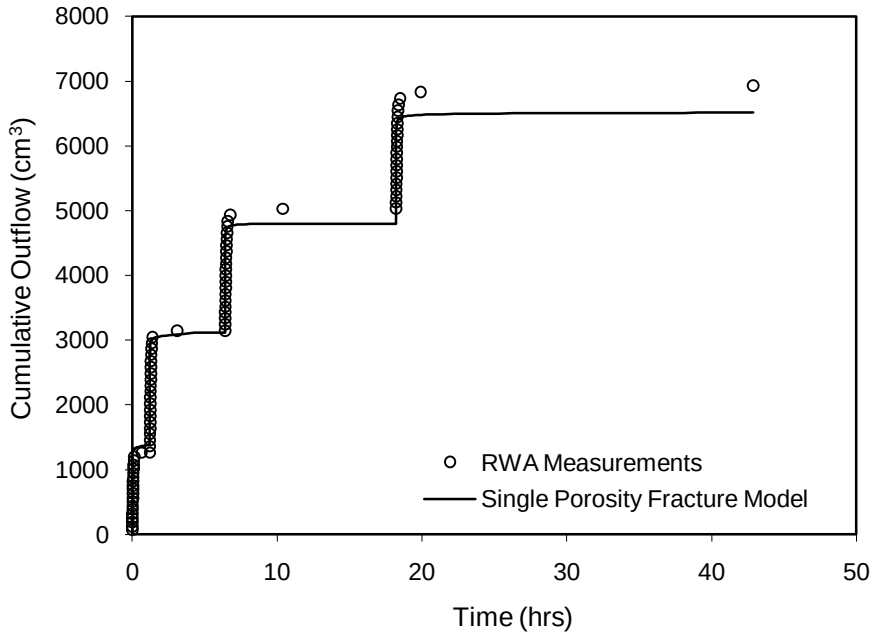

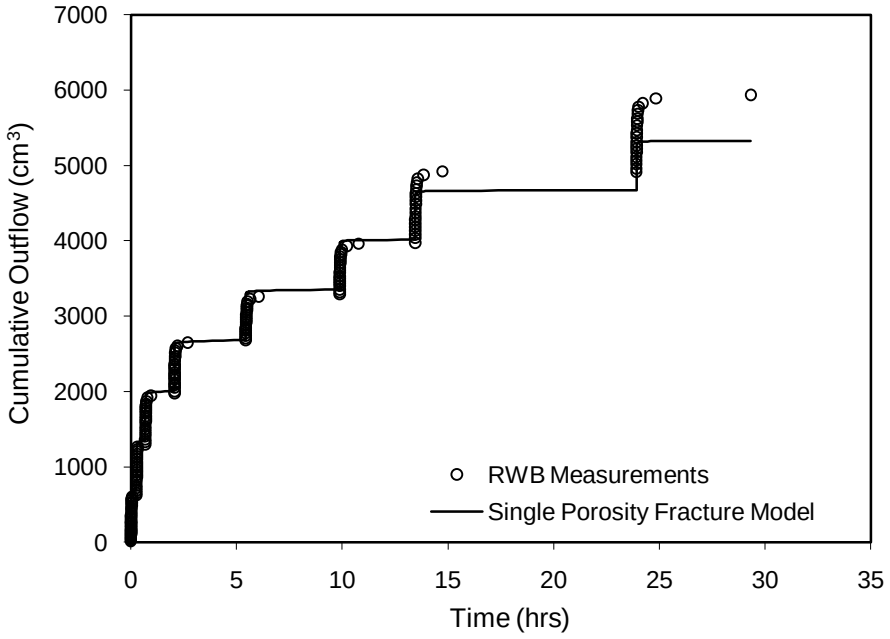

Figure 3.6 Outflow flux data for RWA (upper plot) and RWB (lower plot) with inverse modeling fits using the best fit fracture parameters from Table 3.8. (Figure 3.5 continued on the following page)

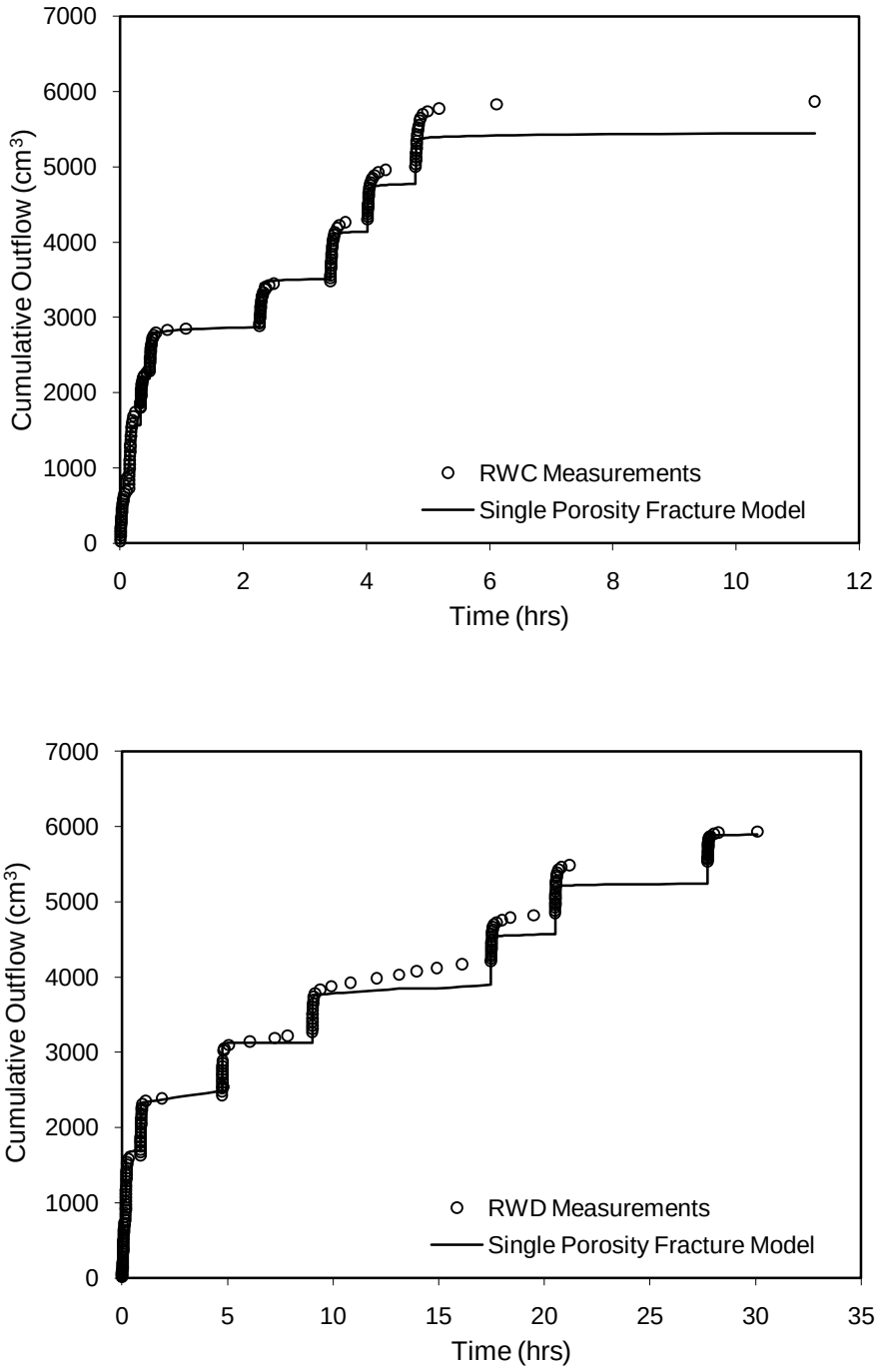

Figure 3.6 Outflow flux data for RWC (upper plot) and RWD (lower plot) with inverse modeling fits using the best fit fracture parameters from Table 3.8.

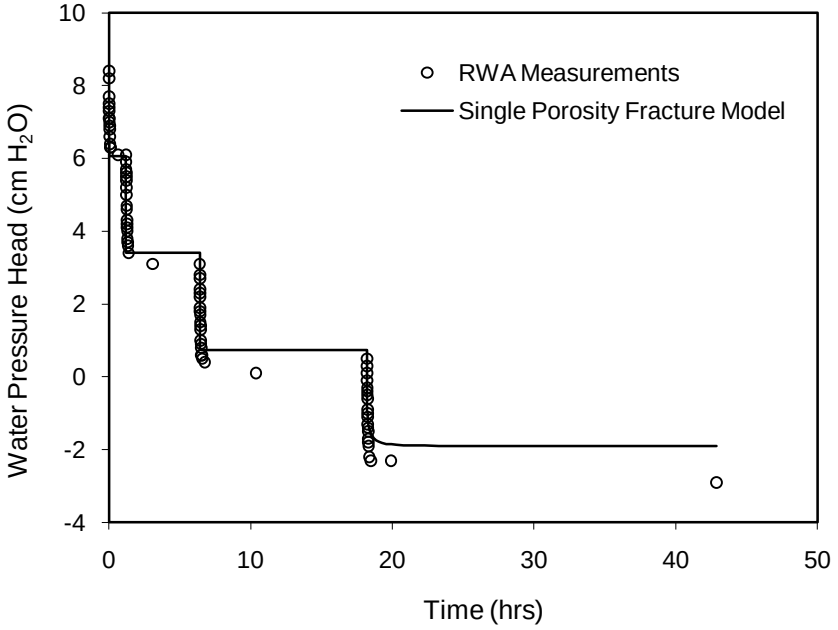

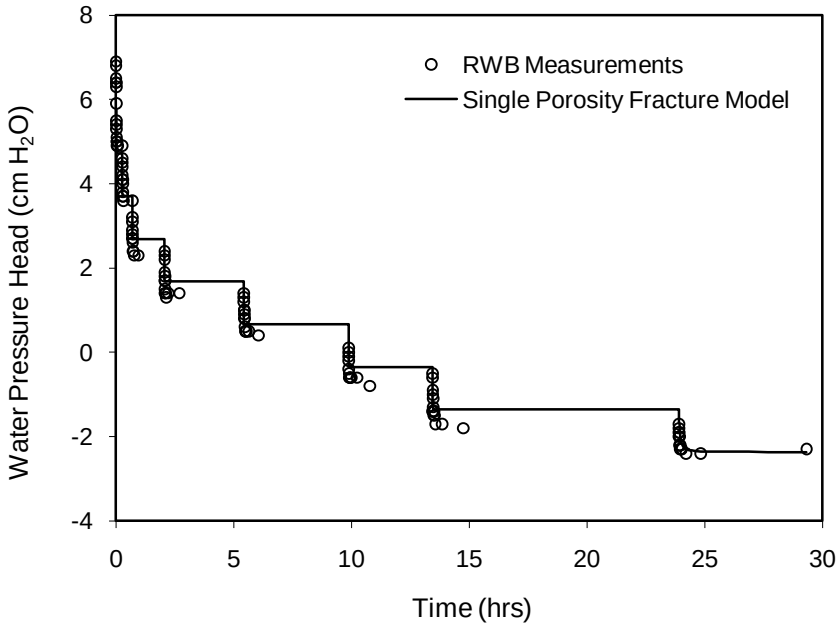

Figure 3.7 Water pressure data for RWA (upper plot) and RWB (lower plot) with inverse modeling fits using the best fit fracture parameters from Table 3.8 (Figure 3.6 continued on the following page)

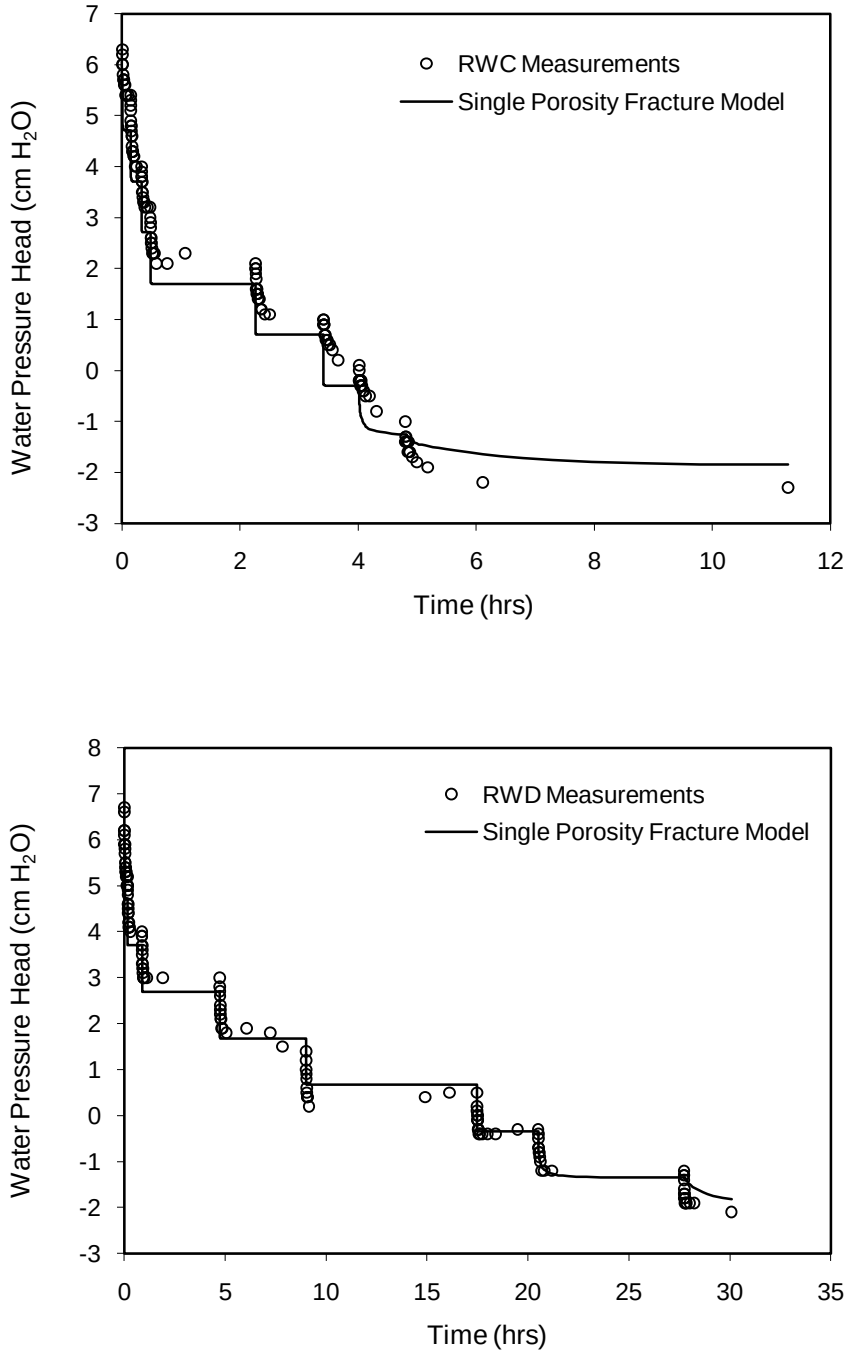

Figure 3.7 Water pressure data for RWC (upper plot) and RWD (lower plot) with inverse modeling fits using the best fit fracture parameters from Table 3.8

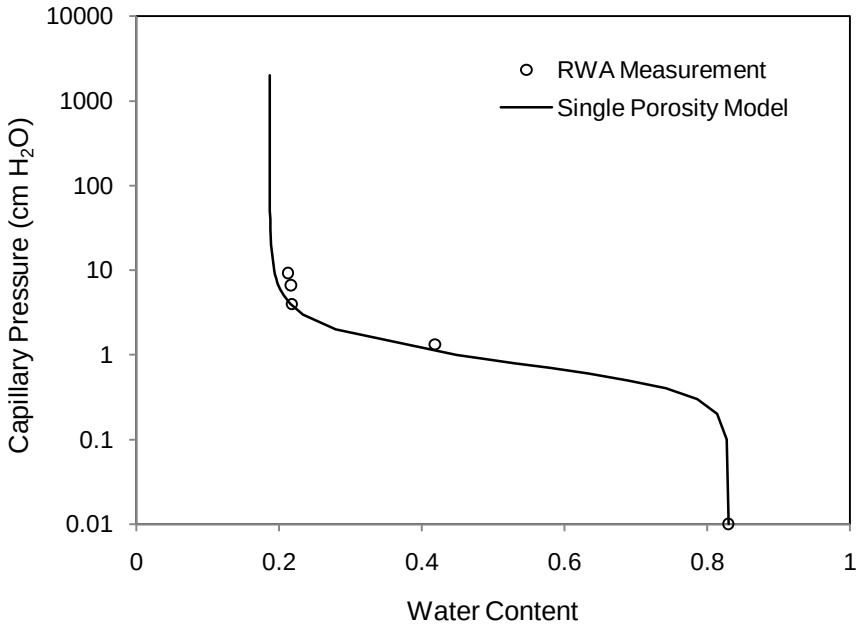

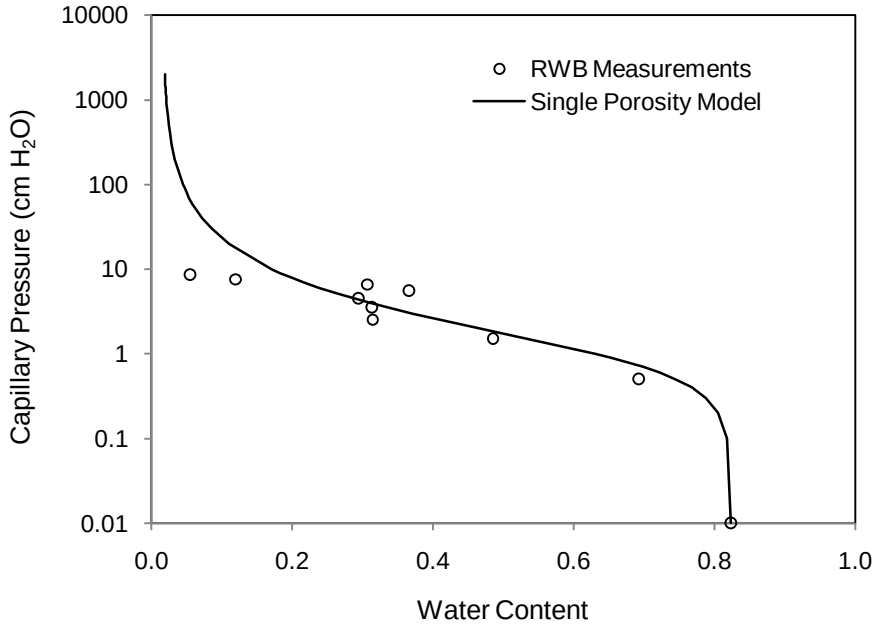

Figure 3.8 The capillary pressure-volumetric water content relationships for RWA (upper plot) and RWB (lower plot). The lines show the best fit model predictions for the single porosity models (Figure 3.7 is continued on the next page)

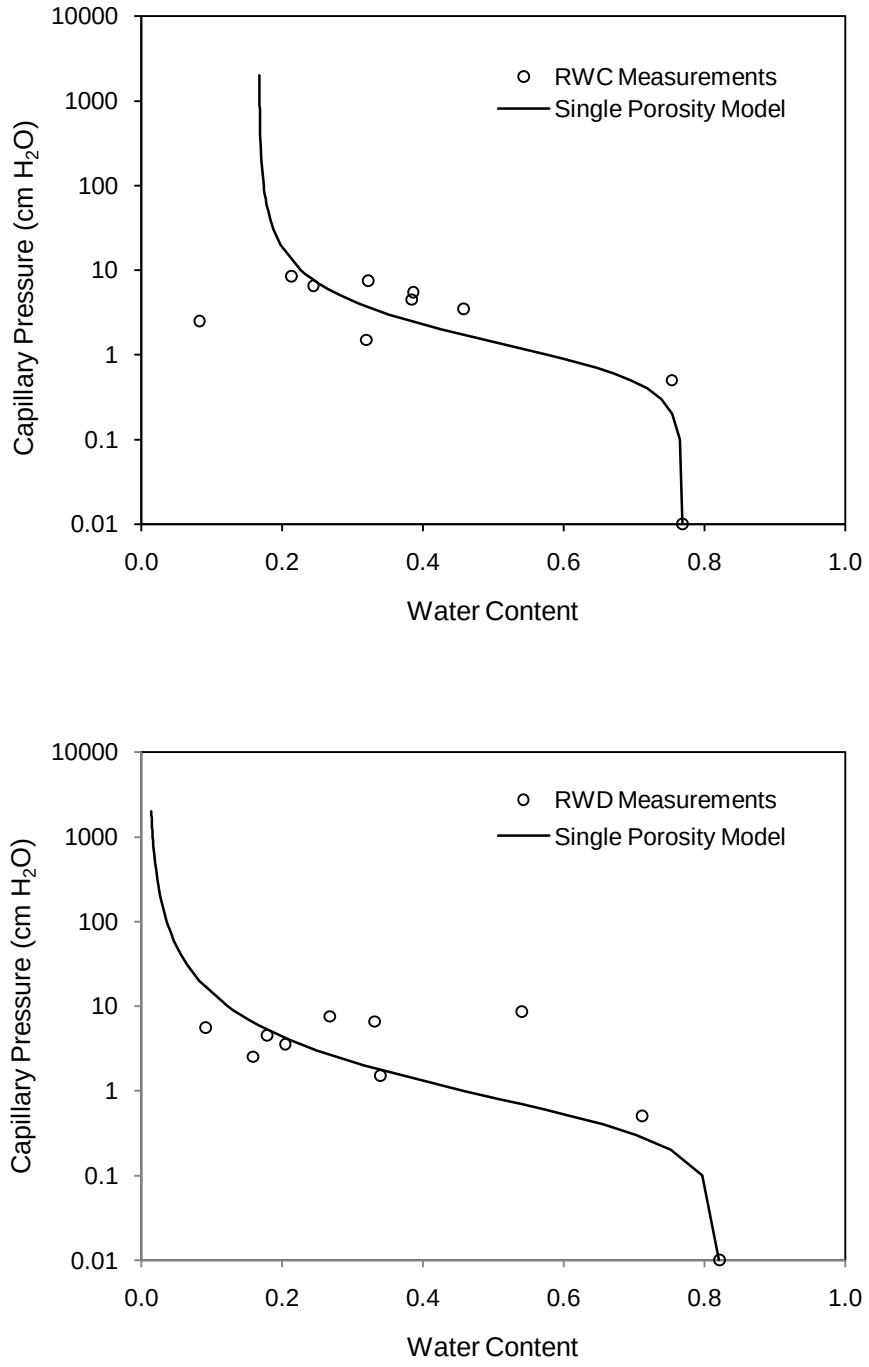

Figure 3.8 The capillary pressure-volumetric water content relationships for RWC (upper plot) and RWD (lower plot). The lines show the best fit model predictions for the single porosity models

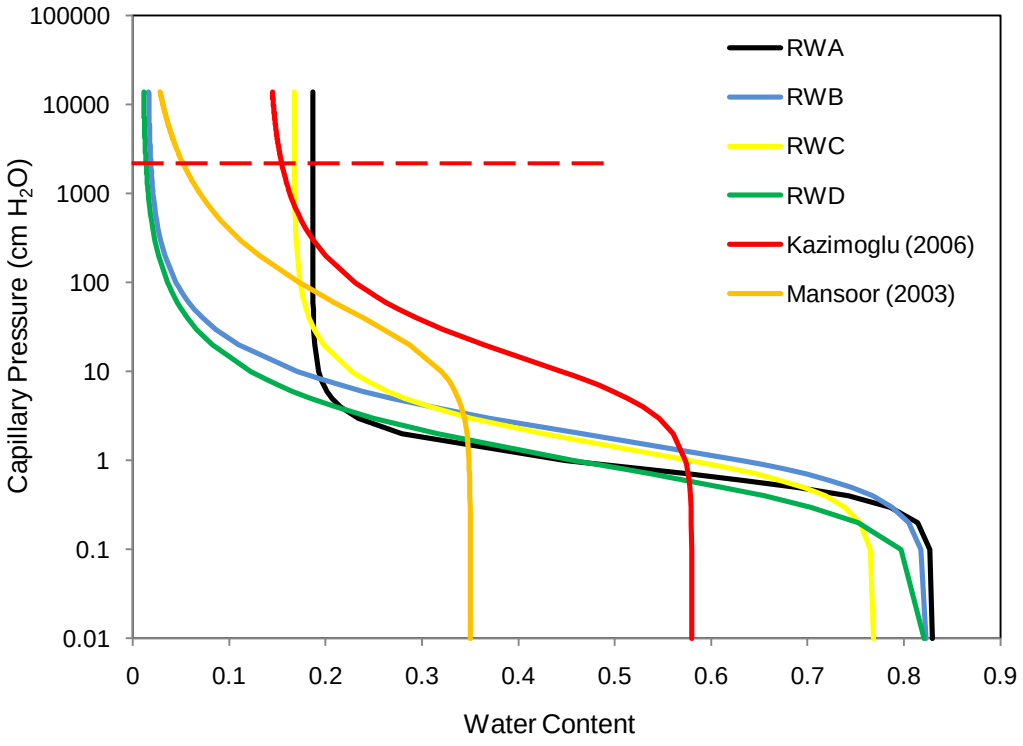

Figure 3.9 Comparison of the capillary pressure-volumetric water content curves developed in this study with curves found in the literature (The red dotted line is an approximation of the highest capillary pressure measured by Kazimoglu, 2006.)

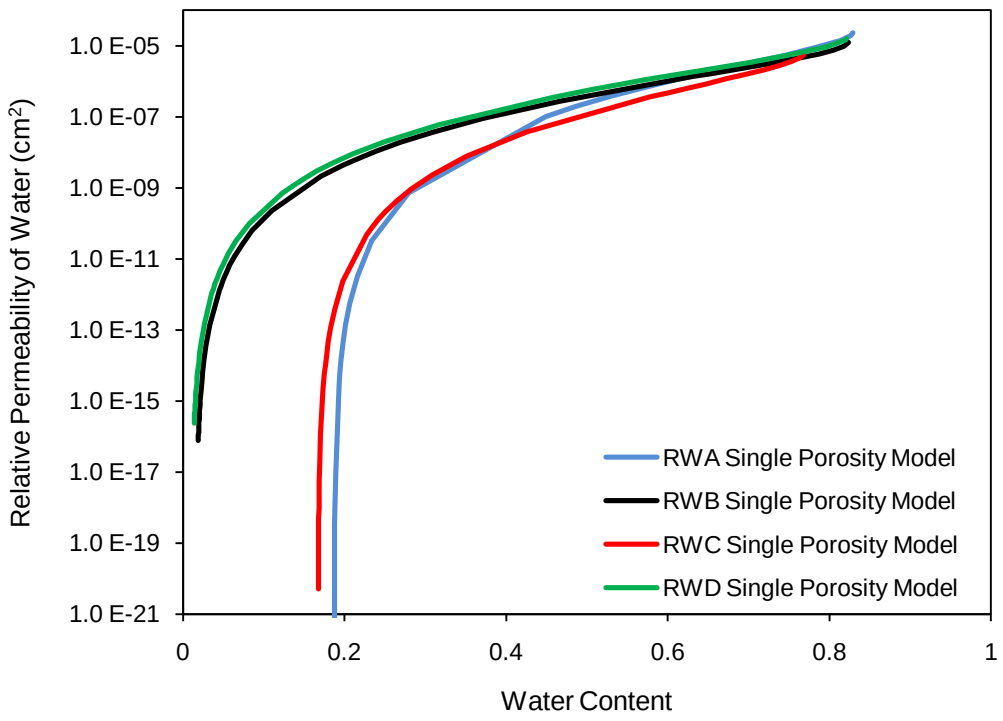

Figure 3.10 Permeability-volumetric water content relationship for the real waste column tests

Chapter 4

CONCLUSIONS

Laboratory tests developed by Han (2009) to obtain constitutive relationships for fluid flow through landfills were run on idealized waste samples as well as real waste samples with the primary objective of determining how the flow properties and constitutive relationships of these samples would be affected by certain changes and comparing the results to similar studies in the literature. Drainage, multi step outflow, saturated hydraulic conductivity and porosity tests were performed on an idealized newspaper sample in order to test the effects of compression. The data obtained from these tests was inversely modeled using HYDRUS-1D and the results were compared to the previous tests performed on newspaper samples by Han (2009).

The set of tests that were run on the newspaper sample helped to reinforce the conclusions drawn by Han (2009) based on previous tests. The first of these conclusions was that if a landfill waste contains a significant amount of paper products or other materials with internal matrix pore domains, the waste is better described by using a dual permeability model instead of a single porosity model. The R^2 values using the dual permeability model were better than those for the single porosity model and the visual fit to the water pressure data was significantly improved. Another conclusion was that materials with similar internal pore structures will have very similar hydraulic properties for the matrix domain, even when the fracture domain is changed. This is supported by the results observed in the test at a higher compression density. Even though the saturated hydraulic conductivity was between 20 and 100

times smaller for the sample at a higher compression, the matrix properties observed were almost identical to those of the previous tests.

The second objective of this study was to apply the methods used for an idealized waste sample to real waste and observe the results and compare them with values found in the literature. Although the testing methods could not be directly applied to real solid waste samples, parts of the methods could be used and modified to obtain results. The drainage, saturated hydraulic conductivity and porosity tests were all used to obtain data that could be inversely modeled using a single porosity model in HYDRUS-1D.

The first observation to be made from the results is that despite controlling the composition and density of the waste samples, there was still some degree of variability in the hydraulic properties of the waste. This is not an unexpected result. Even controlling the composition and density of the waste does not ensure that the samples were the same. While an attempt was made to control particle size distributions for each material and keep them approximately equal for each column, it was not controlled by using sieves. While Han (2009) showed that particle size distribution does not have an effect on the matrix domain of a sample, it can affect the results when only a single porosity model is used. Another possible source of variability comes from the orientation of the waste as it is packed. Even though all four samples were well mixed prior to packing, they will all have at least a slightly different structure in the test cells.

The second important observation to be made is that the small variability in the hydraulic properties of the four waste samples tested in this study was compounded when the results of tests performed by others were compared. The

results of this test were not in strong agreement with the results from Kazimoglu et al. (2006) and Mansoor (2003), which were also not in strong agreement with each other. This disagreement shows that it will be difficult, if not impossible to determine a defined set of flow parameters for solid waste using a single porosity model.

In the future, there are a number of possible modifications or changes that could be made to further understand fluid flow through solid waste. First, very few studies have been done in this area and more are needed before any definitive judgments can be made. It would be interesting to see the results of using the same testing apparatus and methods for a large number of wastes samples with varying compositions. A large set of observations using the same methods and apparatus for different compositions would be beneficial in determining if the variability noted in these few studies is indicative of real landfill conditions or if it is in part due to inherent differences in procedural approaches.

Second, it would be interesting to repeat the tests from this study using either fines, or a higher compaction density, or both. Some of the properties, such as the saturated hydraulic conductivity and porosity, differed slightly from the literature values. The explanation given here was that the differences in packing densities could be causing the discrepancies between the observed and literature values. In order to confirm that the testing methods used in this study are on the right track, it would be valuable to test conditions similar to those in the literature and observe better agreement.

Finally, while the measurements made in this study of the fracture domain are useful and a good place to start, to be able to describe the flow properties of solid

waste using a dual permeability model, it is necessary to develop a testing method which will incorporate not only the fracture domain, but the matrix domain as well.

REFERENCES

Beaven, R. P. (2000). "The hydrogeological and geotechnical properties of household waste in relation to sustainable landfilling." PhD dissertation, Queen Mary and Westfield College, University of London.

Beaven, R.P., and Powrie, W. (1995). "Hydrogeological and geotechnical properties of refuse using a large compression cell." *Proceedings of Sardinia 1995, 5th International Landfill Symposium*, October 2-6, Cagliari, Italy.

Bleiker, E. D., McBean, E., and Farquhar, G. (1993). "Refuse sampling and permeability testing at the Brock Westland Keele Valley landfills." *Proceedings, Sixteenth International Madison Waste Conference: municipal & industrial waste*, September 22-23, 1993, 548-567.

Burrows, M. R., Joseph, J. B., and Mather, J. D. (1997). "The hydraulic properties of in-situ landfilled waste." *Proceedings of Sardinia 1997, 6th International Landfill Symposium*, October 13-17, S. Margarita di Pula, Italy

Chen, T. and Chynoweth, D. P. (1995). "Hydraulic conductivity of compacted municipal solid waste." *Bioresource Technology*, 51, 205-212.

Ciollaro, G., and Romano, N. (1995). "Spatial variability of the hydraulic properties of a volcanic soil." *Geoderma*, 65, 263-282.

Durmusoglu, E., Sanchez, I. M., and Corapcioglu, M. Y. (2006). "Permeability and compression characteristics of municipal solid waste samples." *Environmental Geology*, 50, 773-786.

Fungaroli, A., and Steiner, A. (1979). "Investigation of sanitary landfill behavior, Vols. 1 and 2." USEPA-600/2-79-053a.

Han, B. (2009). "Development of techniques for measuring water and fluid flow properties in solid waste in landfills." PhD dissertation, College of Civil and Environmental Engineering, University of Delaware.

Hopmans, J. W., Grismer, M. E., Chen, J., and Liu, Y. P. (1998). "Parameter estimation of two-fluid capillary pressure-saturation and permeability functions." National Risk Management Research Laboratory, Office of Research and Development, USEPA.

Johnson, C. A., Richner, G. A., Vitvar, T., Schittli, N., and Eberhard, M. (1998). "Hydrological and geochemical factors affecting leachate composition in municipal solid waste incinerator bottom ash Part I: The hydrology of Landfill Lostorf, Switzerland." *Journal of Contaminant Hydrology*, 33, 361-376.

Johnson, C. A., Schaap, M. G., and Abbaspour, K. C. (2001). "Model comparison of flow through a municipal solid waste incinerator ash landfill." *Journal of Hydrology*, 243, 55-72.

Kazimoglu, Y. K., McDougall, J. R., and Pyrah, I. C., (2006) "Unsaturated hydraulic conductivity of landfilled waste." *Proceedings of the 4th International Conference on Unsaturated Soils*, Arizona.

Kodešová, R., Kočárek, M., Kodeš, V., Šimůnek, J., and Kozák, J. (2008). "Impact of soil micromorphological features on water flow and herbicide transport in soils." *Vadose Zone Journal*, 7, 798-809.

Köhne, J. M., Köhne, S., and Gerke, H. H. (2002). "Estimating the hydraulic functions of dual-permeability models from bulk soil data." *Water Resources Research*, 38(7), 26-1.

Korfiatis, G. P., Demetracopoulos, A. C., Bourodimos, E. L., and Nawy, E. G. (1984). "Moisture transport in a solid waste column." *Journal of Environmental Engineering, ASCE*, 110(4), 789-796.

Mansoor, I. (2003). "Applications of soil mechanics principles to landfill waste." PhD dissertation, School of Civil Engineering and the Environment, Southampton University, UK.

Oweis I. S., Smith, D. A., Ellwood, R. B., and Greene, D. (1990) "Hydraulic characteristic of municipal refuse." *Journal of Geotechnical Engineering*, 116(4), 539-553.

Powrie, W. and Beaven, R. P. (1999). "Hydraulic properties of household waste and implications for landfills." *Proceedings of the Institution of Civil Engineers-Geotechnical Engineering*, 137, 235-247.

Reinhart, D. R. and Townsend, T. G. (1998). *Landfill Bioreactor Design and Operation*, Lewis Publishers, Boca Raton.

Rosqvist, N. H., Dollar, L. H., and Fourie, A. B. (2005). "Preferential flow in municipal solid waste and implications for long-term leachate quality: valuation of laboratory-scale experiments." *Waste Management & Research*, 23, 367-380.

Schwärzel, K., Šimůnek, J., Stoffregen, H., Wessolek, G., and van Genuchten, M. T. (2006). "Estimation of the unsaturated hydraulic conductivity of peat soils: laboratory versus field data." *Vadose Zone Journal*, 5(2), 628-640.

Seguin, D., Montillet, A., and Comti, J. (1998). "Experimental characterization of flow regimes in various porous media-I: Limit of laminar flow regime." *Chemical Engineering Science*, 53(21), 3751-3761.

Šimůnek, J., Šejna, M., Saito, H., Sakai, M., and van Genuchten, M. T. (2008). *The HYDRUS-1D Software Package for Simulating the One-Dimensional Movement of Water, Heat, and Multiple Solutes in Variably-Saturated Media (Version 4.0)*, Department of Environmental Sciences, University of California Riverside, Riverside, California.

Šimůnek, J., Wendroth, O., van Genuchten, M. T. (1999) Estimating unsaturated soil hydraulic properties from laboratory tension disc infiltrometer experiments." *Water Resources Research*, 30(10), 2965-2979.

USEPA. (2009). "Municipal Solid Waste Generation, Recycling, and Disposal in the United States: Facts and Figures for 2008." EPA-530-F-009-021.

Wind, G. P. (1968) "Capillary conductivity data estimated by a simple method." *Water in the Unsaturated Zone*, 1, 181-191.

Zardava, K., Powrie, W., and White, J. (2009). "The determination of the moisture retention characteristics of waste materials using vertical drainage experiments." *Third International Workshop "Hydro-Physico-Mechanics of Landfills"*, Braunschweig, Germany, March 10-13.

Appendix A

PICTURES TAKEN WHILE PACKING THE REAL WASTE COLUMNS

Figure A.1 Mixed waste prior to packing

Figure A.2 Mixed waste in the column prior to compression

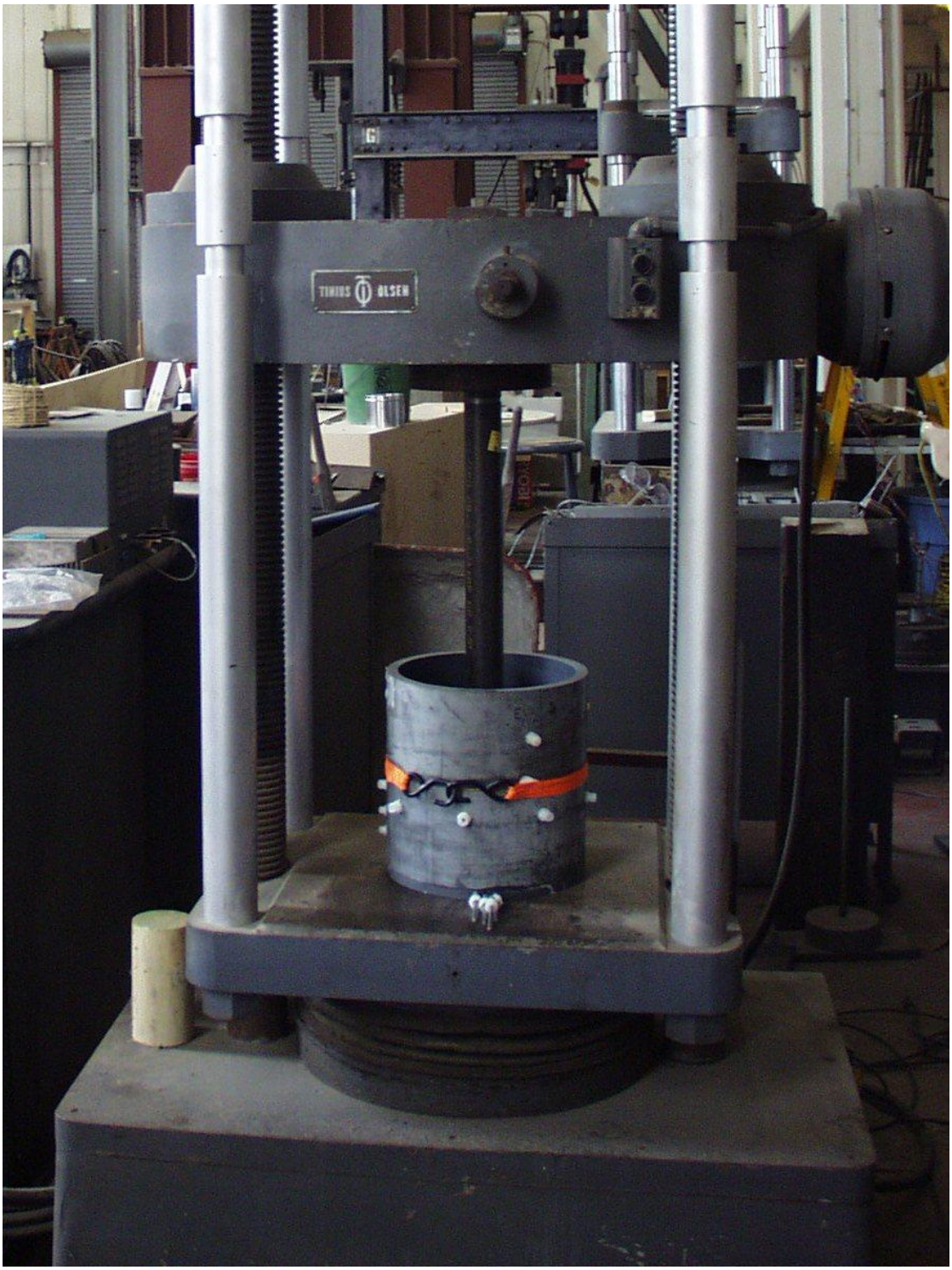

Figure A.3 Compressing the column

Figure A.4 Waste after compression

Figure A.5 Completely compressed waste column with top plate and support rods.